

Joint Resource Allocation and Cache Placement for Location-Aware Multi-User Mobile Edge Computing

Jiechen Chen, Hong Xing, Xiaohui Lin, Arumugam Nallanathan and Suzhi Bi

Abstract

With the growing demand for latency-critical and computation-intensive Internet of Things (IoT) services, mobile edge computing (MEC) has emerged as a promising technique to reinforce the computation capability of the resource-constrained mobile devices. To exploit the cloud-like functions at the network edge, service caching has been implemented to (partially) reuse the computation tasks (e.g., input/output data and program files etc.), thus effectively reducing the delay incurred by data retransmissions and/or the computation burden due to repeated execution of the same task. In a multiuser cache-assisted MEC system, designs for service caching depend on users' preference for different types of services, which is at times highly correlated to the locations where the requests are made. In this paper, we exploit users' location-dependent service preference profiles to formulate a cache placement optimization problem in a multiuser MEC system. Specifically, we consider multiple representative locations, where users at the same location share the same preference profile for a given set of services. In a frequency-division multiple access (FDMA) setup, we jointly optimize the binary cache placement, edge computation resources and bandwidth allocation to minimize the expected weighted-sum energy of the edge server and the users with respect to the users' preference profile, subject to the bandwidth and the computation limitations, and the latency constraints. To effectively solve the mixed-integer non-convex problem, we propose a deep learning based offline cache placement scheme using a novel stochastic quantization based discrete-action generation method. In special cases, we also attain suboptimal caching decisions with low complexity leveraging the structure of the optimal solution. The simulations verify the performance of the proposed scheme and the effectiveness of service caching in general.

Index Terms

Mobile-edge computing, service caching, resource allocation, deep learning.

Part of this paper has been presented at the IEEE International Conference on Communications (ICC), June, 2020 [1].

J. Chen, H. Xing, X. Lin and S. Bi are with the College of Electronics and Information Engineering, Shenzhen University, Shenzhen 518060, China (e-mails: chenjiechen2018@email.szu.edu.cn, {hong.xing, xhlin, bsz}@szu.edu.cn). A. Nallanathan is with the School of Electronic Engineering and Computer Science, Queen Mary University of London, London E1 4NS, U.K. (e-mail: nallanathan@ieee.org).

I. INTRODUCTION

The advent of the Internet of things (IoT) technologies has aroused the proliferation of wireless mobile devices and new applications featuring intensive and real-time computation, such as virtual reality (VR), augmented reality (AR), online gaming, and autonomous driving, etc. [2]. However, fusion of data and service for these emerging types of applications tends to be prohibitive on mobile devices with limited computation capacities. Meanwhile, conventional cloud-based solution such as cloud radio network (CRAN) may incur long transmission delay over the backhaul along with substantial energy cost [3]. To address this issue, fog radio access network (FRAN) has been proposed to provide cloud functionality down to the network edge via cloudlet access points (APs), thus enabling *fog computing* or *mobile edge computing (MEC)* (see [4] and the references therein).

One of the mainstreams on MEC in the literature has centered on joint optimization of communication and computation resource allocation [4–11], such as transmit power, bandwidth and server’s CPU utilization to achieve energy-efficient and low-latency computation. However, the above line of work has not incorporated another dimension of design, *service caching* (or *task caching*). Service caching refers to fetching *a priori* task input data, program files or task results of frequently demanded computation services at edge servers or mobile devices, thus alleviating transmission and execution burden for (partially) repeated request in the future. As a result, service caching further unleashes potential of MEC in terms of energy efficiency and low latency [12–18]. Note that content-oriented caching has been a well-investigated topic aimed for improving user-perceived quality of experience by reducing network congestion, especially for video content delivery (see references [19, 20] and therein). However, there are several different aspects lying between content-oriented and computation-oriented caching. i) Compared with content-oriented caching that mainly fetches data over backhaul, service caching takes place in the shared wireless medium, and is thus more vulnerable to channel hostilities such as channel noise, fading and mutual interference [14, 15]. ii) Computation-oriented tasks are usually context-aware and customized to real-time data generated locally at mobile devices, and therefore the validity of task input/output data and/or program files may last relatively shorter than the content, incurring significant overhead due to service-caching redeployment [12–14].

A. Related Work

There exists rich literature on joint design of communication and computation resource [5–9]. The authors in [5] and [6] considered device-to-device (D2D)-enabled multi-helper MEC systems with multiple tasks, and jointly optimized task offloading and resource allocation to minimize total energy consumption and latency, respectively. In a wireless energy harvesting setup, [7] jointly optimized task offloading decisions and resource allocation assuming binary offloading to maximize the weighted sum computation rate of all users. The total energy consumption was minimized in [8] by joint optimization of resource allocation, partial task offloading policies and energy transmit beamforming at the access point.

On another front, there are also prior work that investigated performance gain brought by service caching. For example, [12] studied a single-user cache-assisted MEC system with dependent tasks, and minimized the average computation latency and energy consumption considering the coupling effect of service cache placement and computation offloading decisions. [13] exploited temporal correlation among sequential task arrivals at a single user to enable proactive caching of partial task results, therefore reducing the total computation energy over a finite time horizon. Furthermore, a multi-user cache-assisted MEC system was considered in [14], where each user requests tasks based on task popularity, and some computation results can be cached and reused in the future at the edge server. Caching decisions and transmission (offloading and downloading) time duration were then jointly optimized to minimize the expected energy cost therein. In addition, [15] assumed that the edge server has the input and the output data of all the computation tasks in a multi-user MEC system. Accordingly, it jointly optimized the local caching decisions of task input and/or output data and computing mode of mobile devices to minimize the transmission bandwidth.

Despite of these previous arts on the integrated design of communication, computation, and caching (3C), some assumed non-casual service demand [12], which may not be valid in practice, as users normally have random request with known or unknown distributions over different types of services. Although some of the work considered users' preference profiles to solve an energy-efficient problem [14] or maximize the expected cumulative number of cache hits [21], they have not taken into account the possible strong correlation between users' preferences and their locations. For example, in an art museum, those who stand in one display spot may have different preferences from those in another display spot. Furthermore, cache placement design

usually involves mixed-integer non-linear programming (MINLP) due to binary caching decision variables, which lacks efficient algorithm to solve in general. Among numerous optimization-based and learning-based methods to solve the MINLP, [22] proposed an integrated learning-optimization framework and demonstrated its high efficiency in tackling the binary offloading problems in MEC networks. However, the effectiveness and scalability for this method to deal with binary cache placement together with (continuous) bandwidth (BW) and computation-capacity allocation is unknown.

To tackle the above challenges, in this paper, we consider a multi-user MEC system equipped with narrow-band wireless communication facilities, where users request delay-sensitive computation services based on their location-dependent preferences. The users are then clustered by a fixed number of locations, and each location is representative of the users who share the service demand profile in common. Then, among the locations that request the same type of service, any user at a location of the best channel condition will be selected to offload the task; and the BS will meet the demand by multicasting the computation results of the service at a rate that ensures successful delivery at all these locations. We aim for minimizing the expected weighted-sum energy consumption with respect to the users' preference profiles by joint optimization of cache placement, edge computation resources, and BW allocations. This problem is subject to instantaneous service deadline constraints, the maximum caching and computation capacities at the BS, as well as the BW constraints for data transmission. To effectively obtain the binary caching decisions, we propose a deep learning (DL) based offline cache placement scheme to solve the one-shot MINLP. The main contributions are summarized as follows.

- We consider multiple representative locations to simplify the problem of multi-user resource allocation and cache placement. This formulation necessitates only the channel state information (CSI) between several locations and the BS, thus facilitates the communications design, and also make the complexity of the problem scale with the number of types of services.
- To obtain an optimal solution to the resource allocation problem given cache placement, we leverage Lagrangian dual decomposition method to solve the problem. The optimization framework used in this stage forms an essential module for the proposed DL-based cache placement policies.
- To solve the MINLP, we propose a DL based offline learning framework, where a deep neural network (DNN) is deployed to learn the cache placement using the synthetic data

samples assuming known distribution of the CSI and task input/output bit-length.

- We propose a novel stochastic quantization based discrete-action generation scheme that samples candidate caching decisions from Bernoulli distribution based on the current model outputs, improving diversity in exploring the optimal caching decisions.
- In special cases when users in one location only request one specified type of service, by exploiting the structure of the optimal solution, we can recast the original problem into a integer linear programming (ILP) and attain suboptimal caching decisions with the complexity reduced to $\mathcal{O}(L^2 \log L)$ using the off-the-shelf software toolboxes.
- Numerical results show the distinguishing performance gain brought by service caching in general and the efficacy of the proposed stochastic quantization based offline cache placement, by comparison with other benchmarks.

The remainder of this paper is organized as follows. The multi-user MEC system model is presented in Section II. Section III formulates the expected weighted-sum energy minimization problem. The jointly optimal solution for communication and computation resource allocation to the problem is investigated in Section IV, with deep learning based offline cache placement proposed in Section V. The special case is studied in Section VI. Numerical results are provided in Section VII. Finally, Section VIII concludes the paper.

Notation—The superscript $([\cdot])^T$ represents the transpose of vectors. $\mathbb{R}^{M \times N}$ stands for the sets of real matrices of dimension $M \times N$. The cardinality of a set is represented by $|\cdot|$. $\text{Exp}(\lambda)$ denotes the exponential distribution with rate parameter λ . $\|\cdot\|$ denotes the Euclidean norm of a vector. In addition, $\text{Pr}(\cdot)$ means the probability of a random event.

II. SYSTEM MODEL

Consider a mobile edge computing (MEC) system equipped with one base station (BS) serving user-ends (UEs) at K different locations (service points) denoted by $\mathcal{K} = \{1, \dots, K\}$. Assume that there is a service library consisting of L independent computation services, denoted by $\mathcal{S} = \{s_1, \dots, s_L\}$. Each computation service is characterized by a three-item tuple (C_l, Q_l, R_l) , $l = 1, \dots, L$. Here, C_l denotes an application-specific computation requirement of the l -th service (in CPU cycles per bit); Q_l and R_l denote the input and output data sizes of the computation service (in bits), respectively. The BS is equipped with a single antenna and an edge server with caching facilities. We assume that all tasks must be executed at the edge server due to limited power and computing resources of the UEs [23]-[24].

A. Location-Aware Task Computation Model

We consider one-shot task requests raised from users at different locations. Specifically, we assume that UEs in one location follow the same task request distributions. We define by a matrix $\mathbf{A} \in \mathbb{R}^{L \times K}$ the tasks' request state, whose (l, k) th entry, $A_{l,k} \in \{0, 1\}$, $s_l \in \mathcal{S}$, $k \in \mathcal{K}$, is given by

$$A_{l,k} = \begin{cases} 1, & \text{if there is a UE at location } k \text{ requesting computation service } s_l, \\ 0, & \text{otherwise.} \end{cases} \quad (1)$$

Also, we denote the fixed probability that at least one UE demands computation service $s_l \in \mathcal{S}$ at location $k \in \mathcal{K}$ as $P_{l,k} = \Pr(A_{l,k} = 1)$, such that $\sum_{s_l \in \mathcal{S}} P_{l,k} = 1$, $\forall k \in \mathcal{K}$.

The BS can proactively cache the computation results of some services to eliminate their real-time execution delay.¹ We define cache placement decisions against service $s_l \in \mathcal{S}$, by an indicator function as follows.

$$I_l = \begin{cases} 1, & \text{if the results of service } s_l \text{ are cached at the BS,} \\ 0, & \text{otherwise.} \end{cases} \quad (2)$$

The maximum caching capacity equipped on the BS is assumed to be S (in bits), i.e.,²

$$\sum_{l=1}^L I_l R_l \leq S. \quad (3)$$

Note that we assume $\sum_{l=1}^L R_l > S$ by default, since the results of all types of services can all be cached otherwise, which reduced to a trivial solution of $I_l = 1, \forall s_l \in \mathcal{S}$.

Under this setup, UEs at different location $k \in \mathcal{K}$ require computation services independently of each other. If the task results for the required services are proactively cached at the BS, the BS will multicast the cached task results to the target UEs. Otherwise, the UEs must first offload the task inputs to and execute the task at the BS.

We define by $\mathcal{K}_l = \{k \in \mathcal{K} | A_{l,k} = 1\}$ the set of locations where UEs demand service $s_l \in \mathcal{S}$. The BS needs to provide the computation result of the l -th service if and only if $|\mathcal{K}_l| \geq 1$, $\forall s_l \in \mathcal{S}$. We adopt a commonly used computation model [13], in which the total number of

¹The delay of proactive offloading and executing the input data is sufficiently small compared with the deadline, and therefore the computation results can be reused for a long period of time in the future.

²We assume a type of on-chip caching facilities that incurs negligible accessing delay, e.g., SRAM, with reading/writing speed of 1.5Gb/s and S around 72Mbits [25].

CPU cycles required for performing one computation task is linearly proportioned to its task input bit length. As a result, the total number of CPU cycles required for the l -th task is given by $C_l Q_l$. We assume a multi-core CPU architecture at the edge server, so that each offloaded task is processed by a different core. Thanks to dynamic voltage and frequency scaling techniques (DVFS) [6], we denote the variable computation frequency (in cycles per second) and the incurred delay for processing the l -th task as f_l and t_l^c , which are related by

$$t_l^c = \begin{cases} \frac{C_l Q_l}{f_l} (1 - I_l), & \text{if } |\mathcal{K}_l| \geq 1, \\ 0, & \text{otherwise.} \end{cases} \quad (4)$$

Notice that we simply set $t_l^c = f_l = 0$ for service s_l with $|\mathcal{K}_l| = 0$. (4) implies that the BS does not need to recompute the cached computation result with $I_l = 1$. The same maximum computation frequency constraints are applied to all the computation cores, i.e.,

$$f_l \leq f_0^{\max}, \quad \forall s_l \in \mathcal{S}. \quad (5)$$

Accordingly, the energy consumed by the BS for executing service s_l is expressed as [13]

$$E_l^c = \begin{cases} \kappa_0 \frac{(C_l Q_l)^3}{(t_l^c)^2} (1 - I_l), & \text{if } |\mathcal{K}_l| \geq 1, \\ 0, & \text{otherwise.} \end{cases} \quad (6)$$

where κ_0 is a constant denoting the effective capacitance coefficient of the server chip architecture. The expected computation energy consumed by the BS for executing task $s_l \in \mathcal{S}$ w.r.t the distribution of $|\mathcal{K}_l|$ is thus given by

$$\mathbb{E}[E_l^c] = 0 \times \Pr(|\mathcal{K}_l| = 0) + \frac{\kappa_0 (C_l Q_l)^3}{(t_l^c)^2} (1 - I_l) (1 - \Pr(|\mathcal{K}_l| = 0)). \quad (7)$$

As $|\mathcal{K}_l| = 0$ means that no UE in any location requests service s_l , $\Pr(|\mathcal{K}_l| = 0)$ is expressed as

$$\Pr(|\mathcal{K}_l| = 0) = \Pr\left(\bigcap_{k=1}^K A_{l,k} = 0\right) = \prod_{k \in \mathcal{K}} (1 - P_{l,k}). \quad (8)$$

Hence, the expected total computation energy for executing all the request tasks is

$$E^c = \sum_{l=1}^L \mathbb{E}[E_l^c] = \sum_{l=1}^L \frac{\kappa_0 (C_l Q_l)^3}{(t_l^c)^2} (1 - I_l) \left(1 - \prod_{k \in \mathcal{K}} (1 - P_{l,k})\right). \quad (9)$$

B. Location-Aware Communication Model

In this subsection, we introduce the communication models for task offloading and results downloading. We assume that task offloading and result downloading phases perform over separate narrow bands with respectively total BW of B (in Hz). The communications for different services occupy orthogonal bandwidth via FDMA. We define the BW allocated to service $s_l \in \mathcal{S}$ for task offloading (results downloading) by $B_l^{\text{off}} = \alpha_l^{\text{off}} B$ ($B_l^{\text{dl}} = \alpha_l^{\text{dl}} B$), where $\alpha_l^{\text{off}}(\alpha_l^{\text{dl}}) \in [0, 1]$ is the proportion of the BW allocated to service s_l , such that $\sum_{s_l \in \mathcal{S}} B_l^{\text{off}} = B$ ($\sum_{s_l \in \mathcal{S}} B_l^{\text{dl}} = B$). In addition, we assume slow fading scenarios, where the wireless channels remain constant during a specified period (shorter than the channel coherence time), which is defined to be as long as several computation deadline. We also assume that UEs in one location are identical in their path-loss factors and small-scale fading. We denote h'_k and g'_k as channel coefficients between location $k \in \mathcal{K}$ and the BS for task offloading and results downloading, respectively. We assume that $h'_k = \sqrt{A_0}(d_0/d_k)^{\gamma/2}h_k$, $g'_k = \sqrt{A_0}(d_0/d_k)^{\gamma/2}g_k$, $k \in \mathcal{K}$, consist of Rayleigh fading with $h_k, g_k \sim \mathcal{CN}(0, 1)$ and multiplicative path loss $\sqrt{A_0}(d_0/d_k)^{\gamma/2}$, where A_0 is the average channel power gain at reference distance d_0 ; d_k is the distance between location k and the BS, and γ denotes the path loss exponent factor. Without loss of generality, we also assume descending orders for the normalized channel gains as $u_1 \geq \dots \geq u_K$, where $u_k = \|h'_k\|^2/(N_0B)$ is the normalized channel gains with N_0 being the power spectral density of the additive white Gaussian noise (AWGN). Besides, we assume $v_{\pi(1)} \geq \dots \geq v_{\pi(K)}$, where $v_{\pi(k)} = \|g'_{\pi(k)}\|^2/(N_0B)$ and $\pi(\cdot)$ denotes a permutation over \mathcal{K} .

1) **Task Offloading.** The achievable rate for offloading task $s_l \in \mathcal{S}$ from any user at location $k \in \mathcal{K}$ is given by

$$r_{l,k}^{\text{off}} = \alpha_l^{\text{off}} B \log_2 \left(1 + \frac{p_k^{\text{off}} u_k}{\alpha_l^{\text{off}}} \right), \quad (10)$$

where p_k^{off} is the transmitting power at location k . The transmission latency due to offloading service $s_l \in \mathcal{S}$ from location $k \in \mathcal{K}$ is thus expressed as

$$t_{l,k}^{\text{off}} = \frac{Q_l}{r_{l,k}^{\text{off}}} (1 - I_l). \quad (11)$$

When $|\mathcal{K}_l| \geq 1$ locations demand the same computation service $s_l \in \mathcal{S}$, we choose the location among \mathcal{K}_l with the best (normalized) channel gain to perform task offloading so as to reduce

the transmission latency and energy consumption. The energy consumed in offloading service $s_l \in \mathcal{S}$ from location $k \in \mathcal{K}_l$ is:

$$E_{l,k}^{\text{off}} = \begin{cases} p_k^{\text{off}} t_{l,k}^{\text{off}}, & \text{if a UE from location } k \text{ performs task offloading of service } s_l, \\ 0, & \text{otherwise.} \end{cases} \quad (12)$$

If a UE from location $k \in \mathcal{K}_l$ is selected to offload service s_l , no user demands service s_l from any locations with larger channel gains to the BS than location k . As a result, the probability that an UE from location k is selected to offload service $s_l \in \mathcal{S}$ is expressed as follows:

$$P_{l,k}^{\text{off}} = \begin{cases} \Pr\left(\left(\bigcap_{j=1}^{k-1} A_{l,j} = 0\right) \cap A_{l,k} = 1\right) = \prod_{j=1}^{k-1} (1 - P_{l,j}) P_{l,k}, & \text{if } k > 1, \\ \Pr(A_{l,1} = 1) = P_{l,1}, & \text{if } k = 1. \end{cases} \quad (13)$$

The corresponding expected energy for offloading service s_l w.r.t task request distribution at location k expressed as

$$\mathbb{E}[E_{l,k}^{\text{off}}] = p_k^{\text{off}} t_{l,k}^{\text{off}} P_{l,k}^{\text{off}}. \quad (14)$$

The total expected task offloading energy w.r.t demand at location $k \in \mathcal{K}$ is thus given by

$$E_k^{\text{off}} = \sum_{l=1}^L \mathbb{E}[E_{k,l}^{\text{off}}] = p_k^{\text{off}} \sum_{l=1}^L t_{l,k}^{\text{off}} P_{l,k}^{\text{off}}. \quad (15)$$

2) Results Downloading. After remote execution of service $s_l \in \mathcal{S}$, the BS transmits back the results to \mathcal{K}_l by multicasting, such that UEs from all these locations can download their desired results. Assuming that location $\pi(k) \in \mathcal{K}_l$ is of the worst normalized channel gain among the locations where service $s_l \in \mathcal{S}$ is requested, the transmission rate that the BS can successfully multicast the results to UEs in \mathcal{K}_l is expressed as

$$r_{l,\pi(k)}^{\text{dl}} = \alpha_l^{\text{dl}} B \log_2 \left(1 + \frac{p_l^{\text{dl}} v_{\pi(k)}}{\alpha_l^{\text{dl}}} \right), \quad (16)$$

where p_l^{dl} is the transmitting power at the BS for service $s_l \in \mathcal{S}$. The transmission latency caused by downloading the results of the l th service using rate $r_{l,\pi(k)}^{\text{dl}}$ is $t_{l,\pi(k)}^{\text{dl}} = R_l / r_{l,\pi(k)}^{\text{dl}}$. The energy consumed by the BS for multicasting service s_l is accordingly given by

$$E_{l,\pi(k)}^{\text{dl}} = \begin{cases} p_l^{\text{dl}} t_{l,\pi(k)}^{\text{dl}}, & \text{if } g_{\pi(k)} = \arg \min_{k \in \mathcal{K}_l} g_k, \\ 0, & \text{otherwise.} \end{cases} \quad (17)$$

Equation (17) implies that the UEs from all locations with smaller channel gains than location $\pi(k)$ (c.f. channel gains sorted in descending order: as $v_{\pi(k+1)} \geq \dots \geq v_{\pi(K)}$) do not demand for

service s_l . Accordingly, the probability of multicasting service s_l 's results at the rate subject to location $\pi(k)$'s channel gain is given by

$$P_{l,\pi(k)}^{\text{dl}} = \begin{cases} \Pr\left(\left(\bigcap_{j=\pi(k+1)}^{\pi(K)} A_{l,j} = 0\right) \cap A_{l,\pi(k)} = 1\right) = \prod_{j=\pi(k+1)}^{\pi(K)} (1 - P_{l,j}) P_{l,\pi(k)}, & \text{if } \pi(k) < \pi(K), \\ \Pr(A_{l,\pi(K)} = 1) = P_{l,\pi(K)}, & \text{if } \pi(k) = \pi(K). \end{cases} \quad (18)$$

The expected energy for multicasting service s_l 's results w.r.t demand profile is

$$E_l^{\text{dl}} = \sum_{k=1}^K \mathbb{E}[E_{l,\pi(k)}^{\text{dl}}] = \sum_{k=1}^K p_l^{\text{dl}} t_{l,\pi(k)}^{\text{dl}} P_{l,\pi(k)}^{\text{dl}}. \quad (19)$$

The total expected transmission energy consumption at the BS is thus given by

$$E^{\text{dl}} = \sum_{l=1}^L \sum_{k=1}^K \mathbb{E}[E_{l,\pi(k)}^{\text{dl}}] = \sum_{l=1}^L \sum_{k=1}^K p_l^{\text{dl}} t_{l,\pi(k)}^{\text{dl}} P_{l,\pi(k)}^{\text{dl}}. \quad (20)$$

III. PROBLEM FORMULATION

In this section, we formulate the energy minimization problem. The expected weighted-sum energy consumed by the BS (E^c and E^{dl}) and all UEs (E_k^{off} 's) are given by $\beta_0(E^c + E^{\text{dl}}) + \sum_{k=1}^K \beta_k E_k^{\text{off}}$, where $\beta_0 \geq 0$ and $\beta_k \geq 0$ ($\beta_0 + \sum_{k \in \mathcal{K}} \beta_k = 1$) are normalized weighted factors (e.g., set according to the relative portion of population or the priority for energy saving). The total latency for delivering service $s_l \in \mathcal{S}$, i.e., $t_{l,k}^{\text{off}} + t_l^c + t_{l,j}^{\text{dl}}$, for all $s_l \in \mathcal{S}$ and $(k, j) \in \mathcal{K}_l \times \mathcal{K}_l$, is subject to an instantaneous deadline constraint T_l .

Remark 3.1: The formulation can be modified to accommodate expected latency constraints by $\mathbb{E}[t_{l,k}^{\text{off}} + t_l^c + t_{l,j}^{\text{dl}}] \leq T_l$, but we consider herein the latency-critical scenarios where the latency constraint for service s_l must hold for every possible combination of $(k, j) \in \mathcal{K}_l \times \mathcal{K}_l$, thus incurring higher energy consumption than the average latency constraints in general.

By denoting $\boldsymbol{\alpha}^{\text{off}} = [\alpha_1^{\text{off}}, \dots, \alpha_L^{\text{off}}]^T$, $\boldsymbol{\alpha}^{\text{dl}} = [\alpha_1^{\text{dl}}, \dots, \alpha_L^{\text{dl}}]^T$, $\mathbf{t}^c = [t_1^c, \dots, t_L^c]^T$, $\mathbf{t}_l^{\text{off}} = [t_{l,1}^{\text{off}}, \dots, t_{l,K}^{\text{off}}]^T$ and $\mathbf{t}_l^{\text{dl}} = [t_{l,\pi(1)}^{\text{dl}}, \dots, t_{l,\pi(K)}^{\text{dl}}]^T$, $s_l \in \mathcal{S}$, the expected weighted-sum energy minimization problem is formulated as:

$$(P0): \underset{\substack{\mathbf{I}, \boldsymbol{\alpha}^{\text{off}}, \boldsymbol{\alpha}^{\text{dl}}, \mathbf{t}^c, \\ \{\mathbf{t}_l^{\text{off}}\}_{s_l \in \mathcal{S}}, \{\mathbf{t}_l^{\text{dl}}\}_{s_l \in \mathcal{S}}}}{\text{Minimize}} \quad \beta_0 (E^c + E^{\text{dl}}) + \sum_{k=1}^K \beta_k E_k^{\text{off}}$$

Subject to (3)

$$t_{l,k}^{\text{off}} + t_l^c + t_{l,j}^{\text{dl}} \leq T_l, \forall s_l \in \mathcal{S}, \forall (k, j) \in \mathcal{K}_l \times \mathcal{K}_l, \quad (21a)$$

$$t_l^c \geq \frac{C_l Q_l (1 - I_l)}{f_0^{\max}}, \forall s_l \in \mathcal{S}, \quad (21b)$$

$$\sum_{s_l \in \mathcal{S}} \alpha_l^{\text{off}} \leq 1, \quad (21c)$$

$$\sum_{s_l \in \mathcal{S}} \alpha_l^{\text{dl}} \leq 1, \quad (21d)$$

$$\alpha_l^{\text{off}} B \log_2 \left(1 + \frac{p_k^{\text{off}} u_k}{\alpha_l^{\text{off}}} \right) \geq \frac{Q_l (1 - I_l)}{t_{l,k}^{\text{off}}}, \forall k \in \mathcal{K}, \forall s_l \in \mathcal{S}, \quad (21e)$$

$$\alpha_l^{\text{dl}} B \log_2 \left(1 + \frac{p_l^{\text{dl}} v_{\pi(k)}}{\alpha_l^{\text{dl}}} \right) \geq \frac{R_l}{t_{l,\pi(k)}^{\text{dl}}}, \forall k \in \mathcal{K}, \forall s_l \in \mathcal{S}, \quad (21f)$$

$$I_l = \{0, 1\}, \alpha_l^{\text{off}} \in [0, 1], \alpha_l^{\text{dl}} \in [0, 1], \forall s_l \in \mathcal{S}. \quad (21g)$$

The constraints in (21b) are obtained by plugging (4) into the maximum frequency constraints (c.f. (5)). Constraints (21c) and (21d) are communication BW constraints for task offloading and results downloading, respectively. It is also worth-noting that constraints (21e) and (21f) are the minimum transmission rate requirements (c.f. (10) and (16)), which can be easily shown to be active when (P0) is optimally solved.

In addition, problem (P0) can be further simplified by merging some of its constraints as follows.

Lemma 3.1: Problem (P0) can be equivalently transformed to the following problem:

$$\begin{aligned} (\text{P0}') : \quad & \underset{\substack{\mathbf{I}, \boldsymbol{\alpha}^{\text{off}}, \boldsymbol{\alpha}^{\text{dl}}, \mathbf{t}^c, \\ \{\mathbf{t}_l^{\text{off}}\}_{s_l \in \mathcal{S}}, \{\mathbf{t}_l^{\text{dl}}\}_{s_l \in \mathcal{S}}}}{\text{Minimize}} \quad \beta_0 (E^c + E^{\text{dl}}) + \sum_{k=1}^K \beta_k E_k^{\text{off}} \\ & \text{Subject to } (3), (21b) - (21g) \\ & t_{l,K}^{\text{off}} + t_l^c + t_{l,\pi(K)}^{\text{dl}} \leq T_l, \forall s_l \in \mathcal{S}. \end{aligned} \quad (22a)$$

Proof: Constraints (21a) include all cases where the transmission and execution delay for any task should be within deadline T . Hence, if the worst case with the longest service latency satisfies the deadline constraint, i.e., $t_{l,K}^{\text{off}} + t_l^c + t_{l,\pi(K)}^{\text{dl}} \leq T_l, \forall s_l \in \mathcal{S}$, so do all other cases.

IV. OPTIMAL COMMUNICATION AND COMPUTATION RESOURCE ALLOCATION

In this section, we study the optimal solution to problem (P0'). Since problem (P0') is a MINLP that is in general NP-hard, we solve (P0') by decomposing it into two-stage optimization problems: 1) BW and edge computing resource allocation problem with the caching decisions

fixed as $\mathbf{I} = \bar{\mathbf{I}}$, denoted as (P0'-1); and 2) cache placement problem (P0'-2) to find the optimal caching decisions. In this section, we focus on solving (P0'-1).

It is easily verified that (P0'-1) is a convex problem (e.g., constraints (21e) and (21f) are perspective of concave functions), and also satisfies Slater's condition. Hence, we leverage Lagrangian dual decomposition method to solve problem (P0'-1) with strong duality guaranteed [26].

By denoting the primal-variable tuple and dual-variable tuple as $\mathbf{P} = (\boldsymbol{\alpha}^{\text{off}}, \boldsymbol{\alpha}^{\text{dl}}, \{\mathbf{t}_l^{\text{dl}}\}, \{\mathbf{t}_l^{\text{off}}\}, \mathbf{t}^c)$ and $\mathbf{D} = (\boldsymbol{\mu}, \boldsymbol{\eta}, \boldsymbol{\omega}, \boldsymbol{\gamma}, \sigma, \epsilon)$, respectively, the (partial) Lagrangian of (P0'-1) is given by

$$\begin{aligned} \mathcal{L}(\mathbf{P}, \mathbf{D}) = & \beta_0 \sum_{l=1}^L \kappa_0 \frac{(C_l Q_l)^3}{(t_l^c)^2} (1 - \bar{I}_l) (1 - \prod_{k=1}^K (1 - P_{l,k})) + \beta_0 \sum_{l=1}^L \sum_{k=1}^K p_l^{\text{dl}} t_{l,\pi(k)}^{\text{dl}} P_{l,\pi(k)}^{\text{dl}} + \sum_{k=1}^K \beta_k p_k^{\text{off}} \\ & \sum_{l=1}^L t_{l,k}^{\text{off}} P_{l,k}^{\text{off}} + \sum_{l=1}^L \mu_l (t_{l,K}^{\text{off}} + t_l^c + t_{l,\pi(K)}^{\text{dl}} - T_l) + \sum_{l=1}^L \eta_l \left(\frac{C_l Q_l (1 - I_l)}{f_0^{\text{max}}} - t_l^c \right) + \sigma \left(\sum_{l=1}^L \alpha_l^{\text{off}} - 1 \right) + \\ & \epsilon \left(\sum_{l=1}^L \alpha_l^{\text{dl}} - 1 \right) + \sum_{k=1}^K \sum_{l=1}^L \omega_{l,k} \left(\frac{Q_l}{t_{l,k}^{\text{off}}} - \alpha_l^{\text{dl}} B \log_2 \left(1 + \frac{p_k^{\text{off}} u_k}{\alpha_l^{\text{off}}} \right) \right) + \sum_{k=1}^K \sum_{l=1}^L \gamma_{l,k} \left(\frac{R_l}{t_{l,\pi(k)}^{\text{dl}}} - \alpha_l^{\text{dl}} B \right. \\ & \left. \log_2 \left(1 + \frac{p_l^{\text{dl}} v_{\pi(k)}}{\alpha_l^{\text{dl}}} \right) \right), \end{aligned} \quad (23)$$

where $\boldsymbol{\mu} = [\mu_1, \dots, \mu_L]^T$, $\boldsymbol{\eta} = [\eta_1, \dots, \eta_L]^T$, $\boldsymbol{\omega} = [\omega_{1,1}, \dots, \omega_{L,K}]^T$ and $\boldsymbol{\gamma} = [\gamma_{1,1}, \dots, \gamma_{L,K}]^T$ denote the Lagrangian dual variables associated with the constraints (22a), (21b), (21e) and (21f), respectively. Dual variables σ and ϵ are, respectively, associated with the two constraints specified in (21c) and (21d). To facilitate primary problem decomposition over s_l , (23) can be equivalently expressed as

$$\begin{aligned} \mathcal{L}'(\mathbf{P}, \mathbf{D}) = & \left(\beta_0 \sum_{l=1}^L \kappa_0 (1 - \bar{I}_l) \frac{(C_l Q_l)^3}{(t_l^c)^2} (1 - \prod_{k=1}^K (1 - P_{l,k})) + \sum_{l=1}^L \mu_l t_l^c - \sum_{l=1}^L \eta_l t_l^c \right) + \left(\beta_0 \sum_{l=1}^L \sum_{k=1}^K \right. \\ & p_l^{\text{dl}} t_{l,\pi(k)}^{\text{dl}} P_{l,\pi(k)}^{\text{dl}} + \sum_{l=1}^L \mu_l t_{l,\pi(K)}^{\text{dl}} + \sum_{k=1}^K \sum_{l=1}^L \gamma_{l,k} \frac{R_l}{t_{l,\pi(k)}^{\text{dl}}} \left. \right) + \left(\sum_{k=1}^K \beta_k p_k^{\text{off}} \sum_{l=1}^L t_{l,k}^{\text{off}} P_{l,k}^{\text{off}} + \sum_{l=1}^L \mu_l t_{l,K}^{\text{off}} + \sum_{k=1}^K \right. \\ & \sum_{l=1}^L \omega_{l,k} \frac{Q_l}{t_{l,k}^{\text{off}}} \left. \right) + \left(\sigma \sum_{l=1}^L \alpha_l^{\text{off}} - \sum_{k=1}^K \sum_{l=1}^L \omega_{l,k} \alpha_l^{\text{dl}} B \log_2 \left(1 + \frac{p_k^{\text{off}} u_k}{\alpha_l^{\text{off}}} \right) \right) + \left(\epsilon \sum_{l=1}^L \alpha_l^{\text{dl}} - \sum_{k=1}^K \sum_{l=1}^L \gamma_{l,k} \alpha_l^{\text{dl}} \right. \\ & \left. B \log_2 \left(1 + \frac{p_l^{\text{dl}} v_{\pi(k)}}{\alpha_l^{\text{dl}}} \right) \right). \end{aligned} \quad (24)$$

The dual function is thus defined as $g(\mathbf{D})$ as follows

$$g(\mathbf{D}) = \min_{\mathbf{P}} \mathcal{L}'(\mathbf{P}, \mathbf{D}) \quad (25)$$

$$\text{Subject to } \alpha_l^{\text{off}} \in [0, 1], \alpha_l^{\text{dl}} \in [0, 1], \forall s_l \in \mathcal{S}.$$

The corresponding dual problem of (P0'-1) is given by

$$(\text{D1}): \text{Maximize } g(\mathbf{D})$$

$$\text{Subject to } \boldsymbol{\mu} \geq 0, \boldsymbol{\eta} \geq 0, \boldsymbol{\omega} \geq 0, \quad (26a)$$

$$\boldsymbol{\gamma} \geq 0, \boldsymbol{\sigma} \geq 0, \boldsymbol{\epsilon} \geq 0. \quad (26b)$$

In the following, we solve problem (P0'-1) by first evaluating (25) given fixed \mathbf{D} , and then iteratively solving problem (D1) to obtain the optimal solution \mathbf{D}^{opt} .

It follows from $\mathcal{L}'(\mathbf{P}, \mathbf{D})$ (c.f. (24)) that problem (25) can be decomposed into the following subproblems over $s_l \in \mathcal{S}$:

$$\min_{t_l^c \geq 0} \beta_0 \kappa_0 (1 - \bar{I}_l) \frac{(C_l Q_l)^3}{(t_l^c)^2} (1 - \prod_{k=1}^K (1 - P_{l,k})) + \mu_l t_l^c - \eta_l t_l^c, \forall s_l \in \mathcal{S}; \quad (27a)$$

$$\begin{cases} \min_{t_{l,\pi(k)}^{\text{dl}} \geq 0} \beta_0 p_l^{\text{dl}} t_{l,\pi(k)}^{\text{dl}} P_{l,\pi(k)}^{\text{dl}} + \gamma_{l,k} \frac{R_l}{t_{l,\pi(k)}^{\text{dl}}}, & \forall s_l \in \mathcal{S}, k \in \mathcal{K} \setminus \{K\}, \\ \min_{t_{l,\pi(k)}^{\text{dl}} \geq 0} \beta_0 p_l^{\text{dl}} t_{l,\pi(k)}^{\text{dl}} P_{l,\pi(k)}^{\text{dl}} + \mu_l t_{l,\pi(k)}^{\text{dl}} + \gamma_{l,k} \frac{R_l}{t_{l,\pi(k)}^{\text{dl}}}, & \forall s_l \in \mathcal{S}, k = K; \end{cases} \quad (27b)$$

$$\begin{cases} \min_{t_{l,k}^{\text{off}} \geq 0} \beta_k p_k^{\text{off}} t_{l,k}^{\text{off}} P_{l,k}^{\text{off}} + \omega_{l,k} \frac{Q_l}{t_{l,k}^{\text{off}}}, & \forall s_l \in \mathcal{S}, k \in \mathcal{K} \setminus \{K\}, \\ \min_{t_{l,k}^{\text{off}} \geq 0} \beta_k p_k^{\text{off}} t_{l,k}^{\text{off}} P_{l,k}^{\text{off}} + \mu_l t_{l,k}^{\text{off}} + \omega_{l,k} \frac{Q_l}{t_{l,k}^{\text{off}}}, & \forall s_l \in \mathcal{S}, k = K; \end{cases} \quad (27c)$$

$$\min_{\alpha_l^{\text{off}} \in [0,1]} \sigma \alpha_l^{\text{off}} - \sum_{k=1}^K \omega_{l,k} \alpha_l^{\text{off}} B \log_2(1 + \frac{p_k^{\text{off}} u_k}{\alpha_l^{\text{off}}}), \forall s_l \in \mathcal{S}; \quad (27d)$$

$$\min_{\alpha_l^{\text{dl}} \in [0,1]} \epsilon \alpha_l^{\text{dl}} - \sum_{k=1}^K \gamma_{l,k} \alpha_l^{\text{dl}} B \log_2(1 + \frac{p_l^{\text{dl}} v_{\pi(k)}}{\alpha_l^{\text{dl}}}), \forall s_l \in \mathcal{S}. \quad (27e)$$

The optimal solution to subproblem (27a)-(27c), denoted by $(\mathbf{t}^c)^*$, $(\mathbf{t}^{\text{dl}})^*$ and $(\mathbf{t}^{\text{off}})^*$ is obtained in the following lemma.

Lemma 4.1: Given fixed \mathbf{D} , the optimal solution to (27a)-(27c), are respectively given by

$$(t_l^c)^* = \begin{cases} \left(\frac{2\beta_0\kappa_0(1-\bar{I}_l)(C_l Q_l)^3(1-\prod_{k=1}^K(1-P_{l,k}))}{\mu_l - \eta_l} \right)^{\frac{1}{3}}, & \text{if } \mu_l - \eta_l > 0, \\ \inf, & \text{otherwise.} \end{cases} \quad (28a)$$

$$(t_{l,\pi(k)}^{\text{dl}})^* = \begin{cases} \sqrt{\frac{\gamma_{l,k} R_l}{\beta_0 p_l^{\text{dl}} P_{l,\pi(k)}^{\text{dl}}}}, & \forall s_l \in \mathcal{S}, k \in \mathcal{K} \setminus \{K\}, \\ \sqrt{\frac{\gamma_{l,k} R_l}{\beta_0 p_l^{\text{dl}} P_{l,\pi(k)}^{\text{dl}} + \mu_l}}, & \forall s_l \in \mathcal{S}, k = K. \end{cases} \quad (28b)$$

$$(t_{l,k}^{\text{off}})^* = \begin{cases} \sqrt{\frac{\omega_{l,k} Q_l}{\beta_k p_k^{\text{off}} P_{l,k}^{\text{off}}}}, & \forall s_l \in \mathcal{S}, k \in \mathcal{K} \setminus \{K\}, \\ \sqrt{\frac{\omega_{l,k} Q_l}{\beta_k p_k^{\text{off}} P_{l,k}^{\text{off}} + \mu_l}}, & \forall s_l \in \mathcal{S}, k = K. \end{cases} \quad (28c)$$

Proof: Please refer to Appendix I.

To solve (27d), we first take the derivative of its objective function w.r.t. α_l^{off} , denoted by $F(\alpha_l^{\text{off}})$, $s_l \in \mathcal{S}$, which is defined as follows:

$$F(\alpha_l^{\text{off}}) = \sum_{k=1}^K \frac{\omega_{l,k} B}{\ln 2} \left(\ln \left(1 + \frac{p_k^{\text{off}} u_k}{\alpha_l^{\text{off}}} \right) - \frac{p_k^{\text{off}} u_k}{\alpha_l^{\text{off}} + p_k^{\text{off}} u_k} \right) - \sigma. \quad (29)$$

It is verified that $F(\alpha_l^{\text{off}})$ is non-increasing w.r.t $\alpha_l^{\text{off}} \in (0, 1]$ with $\lim_{\alpha_l^{\text{off}} \rightarrow 0^+} F(\alpha_l^{\text{off}}) = +\infty > 0$ and $F(1) = \sum_{k=1}^K \frac{\omega_{l,k} B}{\ln 2} \left(\ln \left(1 + p_k^{\text{off}} u_k \right) - \frac{p_k^{\text{off}} u_k}{1 + p_k^{\text{off}} u_k} \right) - \sigma$. Therefore, if $F(1) > 0$, it suggests that $F(\alpha_l^{\text{off}}) > 0$ over $\alpha_l^{\text{off}} \in (0, 1]$, and that the optimal α_l^{off} to (27d) is $(\alpha_l^{\text{off}})^* = 1$; otherwise, there must be some $\tilde{\alpha}_l^{\text{off}} \in (0, 1]$ such that $F(\tilde{\alpha}_l^{\text{off}}) = 0$, which turns out to be the optimal α_l^{off} and can be found numerically via bisection method. To sum up

$$(\alpha_l^{\text{off}})^* = \begin{cases} 1, & \text{if } F(1) > 0, \\ \tilde{\alpha}_l^{\text{off}}, & \text{otherwise.} \end{cases} \quad (30)$$

Applying similar procedure to subproblem (27e), we can also obtain the optimal $(\alpha_l^{\text{dl}})^*, \forall s_l \in \mathcal{S}$.

Next, we begin solving problem (D1). Since (28a) implies that the optimal dual variables satisfy $\mu_l - \eta_l > 0, \forall s_l \in \mathcal{S}$, problem (D1) is recast as below:

$$(\text{D1}') : \text{Maximize } g(\mathbf{D})$$

$$\text{Subject to (26a), (26b),}$$

$$\mu_l - \eta_l > 0, \forall s_l \in \mathcal{S}.$$

As $g(\mathbf{D})$ is convex but non-differentiable, we iteratively solve (D1') by subgradient based methods, e.g., (constrained) ellipsoid method, the algorithm of which is summarized in Algorithm 1 [26].

Algorithm 1: Ellipsoid Method for Problem (D1')

Input : Dual variables $\mathbf{D}^{(0)}$ which is centered at ellipsoid $\mathcal{E}^{(0)} \subset \mathbb{R}^{(2KL+2L+2) \times 1}$ containing the optimal dual solution, $n = 0$

1 **repeat**

- 2 Obtain \mathbf{P}^* based on (28a)-(28c) and (30);
- 3 Update the ellipsoid $\mathcal{E}^{(n+1)}$ based on $\mathcal{E}^{(n)}$ and the subgradient of $g(\mathbf{D}^{(n)})$ w.r.t. the dual variables [26]; and set $\mathbf{D}^{(n+1)}$ as the center of ellipsoid $\mathcal{E}^{(n+1)}$;
- 4 Set $n = n + 1$.

5 **until** the stopping criterion for the ellipsoid method is met;

Output: $\mathbf{D}^{\text{opt}} \leftarrow \mathbf{D}^{(n)}$

It then remains to find the primal-optimal solution to (P0'-1). Since $(t_l^c)^*$, $(t_{l,\pi(k)}^{\text{dl}})^*$, $(t_{l,k}^{\text{off}})^*$, $(\alpha_l^{\text{off}})^*$ and $(\alpha_l^{\text{dl}})^*$, $\forall k \in \mathcal{K}, s_l \in \mathcal{S}$ are unique optimal solution to problem (27a) - (27e), the optimal solution $(t_l^c)^{\text{opt}}$, $(t_{l,\pi(k)}^{\text{dl}})^{\text{opt}}$, $(t_{l,k}^{\text{off}})^{\text{opt}}$ to (P0'-1) can be directly obtained by plugging \mathbf{D}^{opt} into (28a) - (28c), while the optimal solutions $(\alpha_l^{\text{off}})^{\text{opt}}$ and $(\alpha_l^{\text{dl}})^{\text{opt}}$ are numerically attained (c.f. (29)). To sum up, with any (feasible) caching decisions given, problem (P0'-1) can be solved by the dual decomposition method as above.

The optimal solution to (P0') can be found by exhaustive search with high computational complexity of $\mathcal{O}(2^{|\mathcal{S}|})$. To accommodate large number of services $|\mathcal{S}|$ with UEs at different locations having independent request over the service library \mathcal{S} , we propose in general a deep learning based algorithm to find cache placement for (P0') in the next section.

V. DEEP LEARNING BASED OFFLINE CACHE PLACEMENT

In this section, we propose a deep learning-based algorithm to solve (P0'-2) under the assumption that the channel gains and the length of the task-input/output bits remain constant during one specified period, but may vary from one period to another. We consider fixed distance between the service locations and the BS with the channel coefficients distributed as h'_k (g'_k) $\sim \mathcal{CN}(0, A_0(d_0/d_k)^\gamma)$ and thus the normalized channel gains u_k 's (v_k 's) distributed as

$\text{Exp}(\frac{N_0 B}{A_0(d_0/d_k)^\gamma})$ ($\text{Exp}(\frac{N_0 B}{A_0(d_0/d_k)^\gamma})$). We also assume that the input/output bit-length for computation tasks in \mathcal{S} are drawn from uniform distributions denoted as $\mathcal{U}(a, b)$, where a and b are the minimum and maximum bounds of the distributions, respectively. As a result, a sufficient number of data samples composed of quadruples as $(\mathbf{h}^{(t)}, \mathbf{g}^{(t)}, \mathbf{Q}^{(t)}, \mathbf{R}^{(t)})$, where $\mathbf{h}^{(t)} = (u_1, \dots, u_K)^T$, $\mathbf{g}^{(t)} = (v_1, \dots, v_K)^T$, $\mathbf{Q}^{(t)} = (Q_1, \dots, Q_L)^T$, and $\mathbf{R}^{(t)} = (R_1, \dots, R_L)^T$ can be synthesized offline in the t th iteration, while the corresponding caching decisions $\mathbf{I}^{(t)*} = (I_1^{(t)*}, \dots, I_L^{(t)*})^T$ serving as “labels” are generated during the training as going to be introduced shortly. When the training finishes, whenever a change arises in the input quadruple, the trained model can be evaluated to yield the joint solution of resource allocation and cache placement, from which the system will benefit for the rest of the current period.

Mathematically, our goal is to generalize a nonlinear mapping between sample inputs and outputs using an approximation function $f_{\boldsymbol{\theta}^{(t)}}$ parameterized by $\boldsymbol{\theta}^{(t)}$ via a DNN, which is defined as:

$$\dot{\mathbf{I}}^{(t)} = f_{\boldsymbol{\theta}^{(t)}}(\mathbf{h}^{(t)}, \mathbf{g}^{(t)}, \mathbf{Q}^{(t)}, \mathbf{R}^{(t)}). \quad (32)$$

In order to identify the parameter vector $\boldsymbol{\theta}^{(t)}$ for the mapping $f_{\boldsymbol{\theta}^{(t)}}(\mathbf{h}^{(t)}, \mathbf{g}^{(t)}, \mathbf{Q}^{(t)}, \mathbf{R}^{(t)})$, we formulate a learning problem with the empirical risk function denoted by $L(\boldsymbol{\theta}; \mathbf{h}^{(\omega)}, \mathbf{g}^{(\omega)}, \mathbf{Q}^{(\omega)}, \mathbf{R}^{(\omega)})$, which measures the mean-square error (MSE) between the model output $f_{\boldsymbol{\theta}^{(t)}}$ and the (labelled) caching decisions $\mathbf{I}^{(\omega)*}$, where ω denotes the index of the training sample, as follows.

$$(P1) : \underset{\boldsymbol{\theta}}{\text{Minimize}} \mathbb{E}_{\omega} \|\mathbf{I}^{(\omega)*} - f_{\boldsymbol{\theta}^{(t)}}(\mathbf{h}^{(\omega)}, \mathbf{g}^{(\omega)}, \mathbf{Q}^{(\omega)}, \mathbf{R}^{(\omega)})\|^2.$$

The offline learning framework for solving problem (P0'-2) is summarized in Fig. 1. It consists of two alternating stages: service caching decisions (“labels”) generation and DNN based offline training, which are detailed in the following subsections.

A. Service Caching Decision Generation

To find the optimal cache placement for problem (P0'-2) by solving (P0'-1) requires exhaustive search over $J = 2^L$ binary candidates, thus causing complexity of $\mathcal{O}(2^L \times 2(2KL + 2L + 2)^2 \log(\sqrt{\phi}W/\zeta))$, where $2(2KL + 2L + 2)^2$ accounts for the complexity for solving (P0'-1) using Algorithm 1 [27], $W \triangleq \max_{\boldsymbol{\omega} \in \partial g(\mathbf{D}), \mathbf{D} \in \mathcal{E}^{(0)}} \|\boldsymbol{\omega}\|$ is a Lipschitz constant for (25) over the initial ellipsoid $\mathcal{E}^{(0)} = \{\mathbf{D} \mid \|\mathbf{D}\| \leq \sqrt{\gamma}\}$, $\boldsymbol{\omega}$ is a sub-gradient of $g(\mathbf{D})$ over $\mathcal{E}^{(0)}$, and ζ is a parameter controlling the accuracy of the ellipsoid algorithm. To address this challenge, we

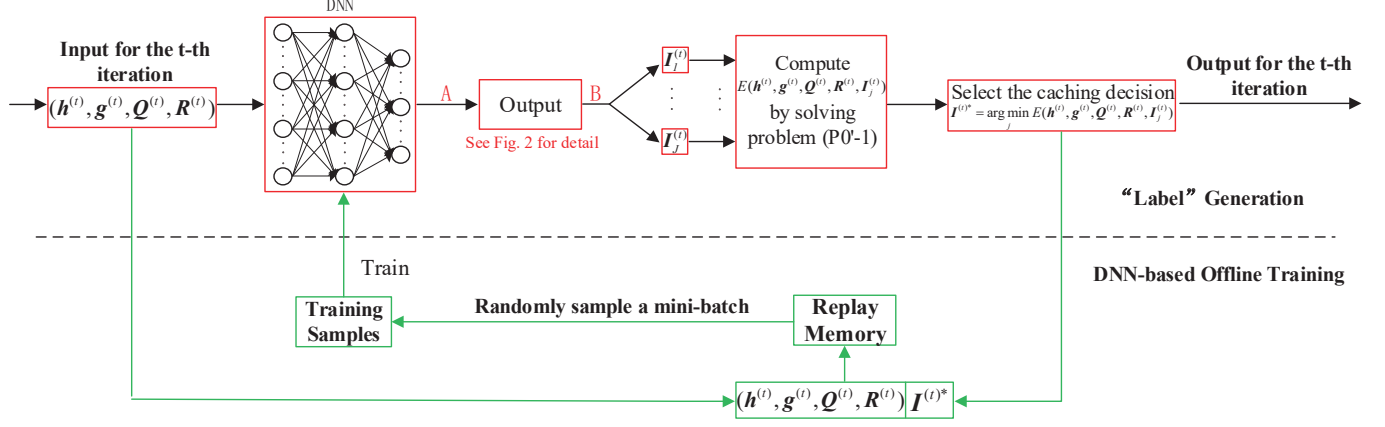


Fig. 1. The offline learning framework for joint resource allocation and cache placement.

propose in this subsection a suboptimal “label” generation scheme that aims for “exploitation” of the current DNN outputs $\dot{\mathbf{I}}^{(t)}$ while providing sufficient diversity for “exploration”. To generate feasible service cache placement, we quantize $\dot{\mathbf{I}}^{(t)}$ into a number J of candidates. Specifically, we propose a stochastic quantization mapping defined as

$$g_J : \dot{\mathbf{I}}^{(t)} \mapsto \{\mathbf{I}_j^{(t)} | \mathbf{I}_j^{(t)} \in \{0, 1\}^L, j = 1, \dots, J\}, \quad (34)$$

which is illustrated in Fig. 2.

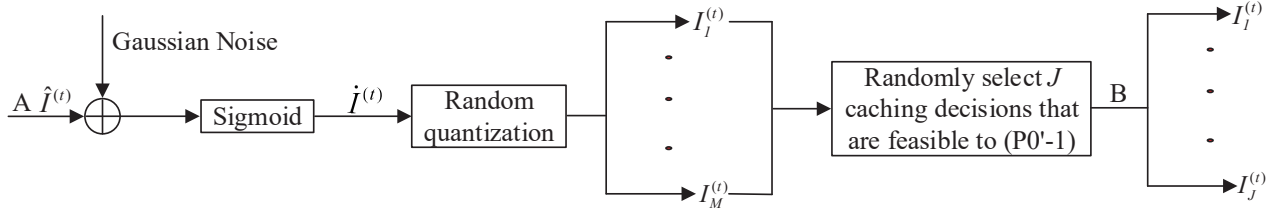


Fig. 2. Gaussian noise-aided stochastic quantization method.

To elaborate, first, we add Gaussian noise to the DNN logits $\hat{\mathbf{I}}^{(t)}$ to generate more diversity in the caching decision space $\{0, 1\}^L$. The sigmoid activation operating on the noisy logits can be, element-wise, expressed as $\dot{\mathbf{I}}^{(t)} = f_{sg}(\hat{\mathbf{I}}^{(t)} + \mathbf{n})$, where $\mathbf{n} \sim \mathcal{N}(0, 1)$, and $f_{sg}(\cdot)$ is the sigmoid function defined by $f_{sg}(x) = 1/(1 + e^{-x})$. Next, we sample from Bernoulli distribution a binary caching decision for each type of the services M times:

$$I_{l,m}^{(t)} = \begin{cases} 1, & \text{with probability } \dot{I}_l^{(t)}, \\ 0, & \text{otherwise,} \end{cases} \quad (35)$$

where $\dot{I}_l^{(t)}$ is the l th entry of $\dot{\mathbf{I}}^{(t)}$, and $I_{l,m}^{(t)}$ denotes the l th entry of the m th candidate $\mathbf{I}_m^{(t)} = (I_{1,m}^{(t)}, \dots, I_{L,m}^{(t)})^T$, $\forall m \in \{1, \dots, M\}$. Finally, we randomly select J ($J < M$) out of M caching decisions that satisfy constraint (3).

Remark 5.1: For the determined order-preserving based caching decisions generation employed in [22], the orders for any two entries are preserved across all M candidates. That is, if $\hat{I}_{l_1}^{(t)} \leq \hat{I}_{l_2}^{(t)}$, then $I_{l_1,m}^{(t)} \leq I_{l_2,m}^{(t)}$ for any $m \in \{1, \dots, M\}$. By comparison, the sampled caching decisions based on (35) provide more uncertainties, and therefore, by properly choosing M and J , it is more likely to find promising candidates satisfying the constraints (3).

Note that any candidate caching decisions violating constraint (3) are discarded. By examining problem (P0'), the caching decisions achieve optimality when constraint (3) is satisfied to its maximum extent.³ Inspired by this, we sort in descending order the entries of 0's in all eligible candidate solutions according to their corresponding value in $\dot{\mathbf{I}}^{(t)}$, and flip 0's to 1's until (3) is satisfied to its maximum extent. Then we evaluate the performance of the J candidate decisions by optimally solving (P0'-1) (see Section IV for detail) using off-the-shelf convex problem solvers such as CVX [28], and the one with the minimum expected energy consumption $E(\mathbf{h}^{(t)}, \mathbf{g}^{(t)}, \mathbf{Q}^{(t)}, \mathbf{R}^{(t)}, \mathbf{I}_j^{(t)})$ will be selected as the caching decision $\mathbf{I}^{(t)*}$ serving as “labels” for problem (P1).

B. Deep Learning Based Offline Training

The newly obtained “label” $\mathbf{I}^{(t)*}$, combined with the sample-inputs $(\mathbf{h}^{(t)}, \mathbf{g}^{(t)}, \mathbf{Q}^{(t)}, \mathbf{R}^{(t)})$, forms a new input-“label” pair $(\mathbf{h}^{(t)}, \mathbf{g}^{(t)}, \mathbf{Q}^{(t)}, \mathbf{R}^{(t)}, \mathbf{I}^{(t)*})$. Specifically, we start with training after sufficient number of input-“label” samples are collected in memory, and update the parameter vector $\boldsymbol{\theta}^{(t)}$ every τ iteration by a stochastic gradient descent (SGD) step as follows

$$\boldsymbol{\theta}^{(t+1)} = \boldsymbol{\theta}^{(t)} - \eta^{(t)} \hat{\nabla} L(\boldsymbol{\theta}^{(t)}), \quad (36)$$

where $\eta^{(t)}$ is the learning rate, and $\hat{\nabla} L(\boldsymbol{\theta}^{(t)}) = \frac{1}{|\mathcal{D}^{(t)}|} \sum_{\omega \in \mathcal{D}^{(t)}} \nabla L(\boldsymbol{\theta}^{(t)}; \mathbf{h}^{(\omega)}, \mathbf{g}^{(\omega)}, \mathbf{Q}^{(\omega)}, \mathbf{R}^{(\omega)})$ is the stochastic gradient approximating $\mathbb{E}_{\omega}[\nabla L(\boldsymbol{\theta}^{(t)}; \mathbf{h}^{(\omega)}, \mathbf{g}^{(\omega)}, \mathbf{Q}^{(\omega)}, \mathbf{R}^{(\omega)})]$ via a mini-batch $\mathcal{D}^{(t)}$ of samples from the memory in the t th iteration. Furthermore, we also maintain the memory with limited capacity (replay memory), where only the latest $|\mathcal{R}|$ input-“label” pairs are kept

³The constraint (3) being satisfied to its maximum extent refers to caching decisions that are feasible to problem (P0'), but incurs violation of (3) if any more type of service is cached.

Algorithm 2: Deep Learning Based Offline Cache Placement

```

1 Initialize the parameter vector  $\theta^{(0)}$ ;
2 repeat
    Input : Wireless channel gains  $\mathbf{h}^{(t)}$  and  $\mathbf{g}^{(t)}$ , service input-bit size  $\mathbf{Q}^{(t)}$  and
              output-bit size  $\mathbf{R}^{(t)}$  at each iteration  $t$ 
3   Obtain the model output  $\dot{\mathbf{I}}^{(t)} = f_{\theta^{(t)}}(\mathbf{h}^{(t)}, \mathbf{g}^{(t)}, \mathbf{Q}^{(t)}, \mathbf{R}^{(t)})$ ;
4   Generate a set of  $J$  feasible caching decisions  $\mathbf{I}_j^{(t)} = g_J(\dot{\mathbf{I}}^{(t)}), \forall j \in \{1, \dots, J\}$ ;
5   Compute  $E(\mathbf{h}^{(t)}, \mathbf{g}^{(t)}, \mathbf{Q}^{(t)}, \mathbf{R}^{(t)}, \mathbf{I}_j^{(t)})$  for all  $\mathbf{I}_j^{(t)}$  by solving (P0'-1);
6   Select the best caching decision  $\mathbf{I}^{(t)*} = \arg \min_j E(\mathbf{h}^{(t)}, \mathbf{g}^{(t)}, \mathbf{Q}^{(t)}, \mathbf{R}^{(t)}, \mathbf{I}_j^{(t)})$ ;
7   Feed the replay memory using the newly collected input-“label” pair
       $(\mathbf{h}^{(t)}, \mathbf{g}^{(t)}, \mathbf{Q}^{(t)}, \mathbf{R}^{(t)}, \mathbf{I}^{(t)*})$ ;
8   if  $t \bmod \tau = 0$  then
9       Randomly sample a mini-batch  $\mathcal{D}^{(t)}$  of samples
           $\{(\mathbf{h}^{(\omega)}, \mathbf{g}^{(\omega)}, \mathbf{Q}^{(\omega)}, \mathbf{R}^{(\omega)}, \mathbf{I}^{(\omega)*}) | \omega \in \mathcal{D}^{(t)}\}$  from the replay memory;
10      Update  $\theta^{(t)}$  by a SGD step (c.f. (36));
11  end
12 until the algorithm converges;

```

for model updates. The overall deep learning based cache placement algorithm is summarized in Algorithm 2.

After the training converges, given any input $(\mathbf{h}^{(t)}, \mathbf{g}^{(t)}, \mathbf{Q}^{(t)}, \mathbf{R}^{(t)})$, the caching decisions can be obtained by implementing steps 3 - 6 in Algorithm 2.

Remark 5.2: While the proposed scheme can be applied to offline sample collection where all the input samples $(\mathbf{h}^{(t)}, \mathbf{g}^{(t)}, \mathbf{Q}^{(t)}, \mathbf{R}^{(t)})$'s can be generated *a priori* based on their known distributions, it can serve as, without loss of generality, an online training framework to accommodate real-time input-sample arrivals with arbitrarily stable (possibly unknown) distributions regarding the channel gains and the service input/output bit-length.

VI. SPECIAL CASE

Consider special scenarios in which UEs at each location demand a unique type of service in $\mathcal{S}' = \{s_1, \dots, s_K\} \subseteq \mathcal{S}$.⁴ This is equivalent to $P_{l,k} = 1$ for $s_l = s_k$ and $P_{l,k} = 0$ for $s_l \in \mathcal{S}' \setminus \{s_k\}$, $\forall k \in \mathcal{K}$. Indices l and k thus become interchangeable. Hence, E^c is recast as $\sum_{k \in \mathcal{K}} \kappa_0 (C_k Q_k)^3 (1 - I_k) / (t_k^c)^2$ (c.f. (9)); E_k^{off} reduces to $p_k^{\text{off}} t_k^{\text{off}} (1 - I_k)$ (c.f. (15)); and E^{dl} is simplified as $\sum_{k \in \mathcal{K}} t_k^{\text{dl}} p_k^{\text{dl}}$ (c.f. (20)). In addition, constraints (21a) also reduce to $t_k^{\text{off}} + t_k^c + t_k^{\text{dl}} \leq T_k, k \in \mathcal{K}$. By denoting $\mathbf{I} = [I_1, \dots, I_K]^T$, $\boldsymbol{\alpha}^{\text{off}} = [\alpha_1^{\text{off}}, \dots, \alpha_K^{\text{off}}]^T$, $\boldsymbol{\alpha}^{\text{dl}} = [\alpha_1^{\text{dl}}, \dots, \alpha_K^{\text{dl}}]^T$, $\mathbf{t}^c = [t_1^c, \dots, t_K^c]^T$, $\mathbf{t}^{\text{off}} = [t_1^{\text{off}}, \dots, t_K^{\text{off}}]^T$ and $\mathbf{t}^{\text{dl}} = [t_1^{\text{dl}}, \dots, t_K^{\text{dl}}]^T$, the weighted-sum energy minimization problem under this special circumstance is formulated as [1]

$$\begin{aligned} \text{(P2): Minimize } & \beta_0 \sum_{k \in \mathcal{K}} \left(\kappa_0 \frac{(C_k Q_k)^3 (1 - I_k)}{(t_k^c)^2} + t_k^{\text{dl}} p_k^{\text{dl}} \right) + \sum_{k \in \mathcal{K}} \beta_k p_k^{\text{off}} t_k^{\text{off}} \\ & \mathbf{I}, \boldsymbol{\alpha}^{\text{off}}, \boldsymbol{\alpha}^{\text{dl}} \\ & \mathbf{t}^c, \mathbf{t}^{\text{dl}}, \mathbf{t}^{\text{off}} \end{aligned} \quad \text{Subject to } \sum_{k=1}^K I_k R_k \leq S, \quad (37a)$$

$$t_k^{\text{off}} + t_k^c + t_k^{\text{dl}} \leq T_k, \forall k \in \mathcal{K}, \quad (37b)$$

$$t_k^c \geq \frac{C_k Q_k (1 - I_k)}{f_0^{\max}}, \forall k \in \mathcal{K}, \quad (37c)$$

$$\sum_{k \in \mathcal{K}} \alpha_k^{\text{off}} \leq 1, \quad (37d)$$

$$\sum_{k \in \mathcal{K}} \alpha_k^{\text{dl}} \leq 1, \quad (37e)$$

$$\alpha_k^{\text{off}} B \log_2 \left(1 + \frac{p_k^{\text{off}} u_k}{\alpha_k^{\text{off}}} \right) \geq \frac{Q_k (1 - I_k)}{t_k^{\text{off}}}, \forall k \in \mathcal{K}, \quad (37f)$$

$$\alpha_k^{\text{dl}} B \log_2 \left(1 + \frac{p_k^{\text{dl}} v_k}{\alpha_k^{\text{dl}}} \right) \geq \frac{R_k}{t_k^{\text{dl}}}, \forall k \in \mathcal{K}, \quad (37g)$$

$$I_k \in \{0, 1\}, \alpha_k^{\text{off}} \in [0, 1], \alpha_k^{\text{dl}} \in [0, 1], \forall k \in \mathcal{K}. \quad (37h)$$

We then provide analytical solution in semi-closed form for the special-case problem (P2) and draw some insights therein. With the caching decisions fixed as $\mathbf{I} = \bar{\mathbf{I}}$, problem (P2) reduces to (P2-1), whose Karush-Kuhn-Tucker (KKT) solution is obtained leveraging the following lemma.

Lemma 6.1: By denoting the Lagrangian multiplier associated with constraints (37b), (37c), (37f), (37g), (37d) and (37e), by $\boldsymbol{\mu} = [\mu_1, \dots, \mu_K]^T$, $\boldsymbol{\eta} = [\eta_1, \dots, \eta_K]^T$, $\boldsymbol{\omega} = [\omega_1, \dots, \omega_K]^T$,

⁴Take mobile VR delivery in a museum as an example, in which users who are located near the same display sharing the same field of vision thus demand and are served by the same task results.

$\gamma = [\gamma_1, \dots, \gamma_K]^T$, σ and ϵ , respectively, the KKT solution to problem (P2-1) for given $(\mu, \eta, \omega, \gamma, \sigma, \epsilon)$ is as follows:

$$(t_k^{\text{dl}})^* = \sqrt{\frac{\gamma_k R_k}{\beta_0 p_k^{\text{dl}} + \mu_k}}, \quad (38a)$$

$$(t_k^{\text{off}})^* = \sqrt{\frac{\omega_k Q_k (1 - \bar{I}_k)}{\beta_k p_k^{\text{off}} + \mu_k}}, \quad (38b)$$

$$(t_k^c)^* = \begin{cases} \left(\frac{2\kappa_0 \beta_0 (1 - \bar{I}_k) (C_k Q_k)^3}{\mu_k - \eta_k} \right)^{\frac{1}{3}}, & \text{if } \mu_k - \eta_k > 0, \\ \inf, & \text{otherwise,} \end{cases} \quad (38c)$$

$$(\alpha_k^{\text{off}})^* = \min \left\{ \frac{p_k^{\text{off}} u_k}{e^{[W_0(-e^{\phi_k \ln 2}) - \phi_k \ln 2]} - 1}, 1 \right\}, \quad (38d)$$

$$(\alpha_k^{\text{dl}})^* = \min \left\{ \frac{p_k^{\text{dl}} v_k}{e^{[W_0(-e^{\varphi_k \ln 2}) - \varphi_k \ln 2]} - 1}, 1 \right\}, \quad (38e)$$

where $W_0(\cdot)$ is the principal branch of Lambert W function defined as the inverse function of $xe^x = y$ [29], $\phi_k = -\frac{\sigma}{\omega_k B} - \frac{1}{\ln 2}$, and $\varphi_k = -\frac{\epsilon}{\gamma_k B} - \frac{1}{\ln 2}$.

Proof: Please refer to [1, Appendix 1].

Remark 6.1: Compared with KKT solution to problem (P0'-1) (cf. (28a) - (28c) and (30)), the optimal offloading/downloading BW for given dual variables can be obtained in semi-closed forms, from which we have the following observations. 1) With the transmitting power p_k^{off} of UEs at location k fixed, the $(\alpha_k^{\text{off}})^*$ of BW allocated for these UEs for offloading is proportional to their channel gain h_k to the BS, and when h_k increases to be larger than a threshold $\frac{e^{[W_0(-e^{\phi_k \ln 2}) - \phi_k \ln 2]} - 1}{p_k^{\text{off}}}$, UEs at location k will gain access to full BW to save transmission latency and thus energy. 2) Likewise, $(\alpha_k^{\text{off}})^*$ is also increasing with p_k^{off} such that the UEs with larger transmitting power are able to finish task offloading faster to save energy. Similar insights can also be drawn from (38e).

Note that for the special-case problem (P2) only, we propose an ILP-based suboptimal cache placement scheme leveraging the KKT solution for BW allocation given by (38d) and (38e). First, provided that the computation frequency of the edge server is fully used for each computation task, e.g., $f_k = f_0^{\text{max}}$, $\forall k \in \mathcal{K}$, the execution delay of any task is thus assumed to be shorter than the deadline for the purpose of energy saving, i.e., $t_k^{\text{off}} + t_k^c + t_k^{\text{dl}} < T$, $\forall k \in \mathcal{K}$. The optimal dual variables associated with constraints (37b) thus become zero due to the complementary slackness. Then assuming that there is no cache placed for any tasks, i.e., $I_k = 0$, $\forall k \in \mathcal{K}$, we substitute (38b) and (38d) for t_k^{off} and α_k^{off} , respectively, in (37d) and (37f). Since it is easy to

verify that (37d) and (37f) are achieved active for optimal solution to (P2-1), this implies a set of equations as follows.

$$\begin{cases} f(\omega_k, \sigma) = \frac{B p_k^{\text{off}} u_k}{\ln 2 \sqrt{O_k \beta_k p_k^{\text{off}}}} - \frac{\exp \left(W_0 \left(-\exp(\phi_k(\omega_k, \sigma) \ln 2) \right) - \phi_k(\omega_k, \sigma) \ln 2 \right) - 1}{\left(W_0 \left(-\exp(\phi_k(\omega_k, \sigma) \ln 2) \right) - \phi_k(\omega_k, \sigma) \ln 2 \right) \sqrt{\omega_k}} = 0, \forall k \in \mathcal{K}, \\ g(\omega_1, \dots, \omega_K, \sigma) = \sum_{k \in \mathcal{K}} \frac{p_k^{\text{off}} u_k}{\exp \left(W_0 \left(-\exp(\phi_k(\omega_k, \sigma) \ln 2) \right) - \phi_k(\omega_k, \sigma) \ln 2 \right) - 1} - 1 = 0. \end{cases} \quad (39)$$

Lemma 6.2: There must exist numerical solutions of σ and ω_k , $\forall k \in \mathcal{K}$ to the set of equations in (39).

Proof: $f(\omega_k, \sigma)$ and $g(\omega_1, \dots, \omega_K, \sigma)$ are both non-decreasing w.r.t ω_k and non-increasing w.r.t σ , $\forall k \in \mathcal{K}$ (Please refer to [1, Appendix 2]). Moreover, it is easily verified that $\lim_{\omega_k \rightarrow 0^+} f(\omega_k, \sigma) = -\infty < 0$, $k \in \mathcal{K}$, and $\lim_{\sigma \rightarrow 0^+} g(\omega_1, \dots, \omega_K, \sigma) = +\infty > 0$. Based on the monotonicity of the two functions, we use bi-section method to solve $f(\omega_k, \sigma) = 0$ by fixing σ , and then plug the solution ω_k , $\forall k \in \mathcal{K}$, into $g(\omega_1, \dots, \omega_K, \sigma)$ to further find σ via bi-section until $g(\omega_1, \dots, \omega_K, \sigma) = 0$ is met.

We can solve another similar set of equations as (39) to obtain optimal ϵ and γ_k , $\forall k \in \mathcal{K}$. Then with $(\alpha_k^{\text{off}})^*$'s and $(\alpha_k^{\text{dl}})^*$'s numerically obtained (c.f. (38d) and (38e)), $t_k^c = \frac{C_k Q_k}{f_0^{\text{max}}}$, t_k^{off} (c.f. (37f)) and t_k^{dl} (c.f. (37g)), $k \in \mathcal{K}$, are obtained as constants, denoted by \bar{t}_k^c , \bar{t}_k^{off} and \bar{t}_k^{dl} , respectively. As a result, problem (P2) reduces to an ILP, with only the caching decision \mathbf{I} as optimization variables as follows:

$$\begin{aligned} \text{(P2-2):} \quad & \underset{\mathbf{I}}{\text{Minimize}} \quad \beta_0 \sum_{k \in \mathcal{K}} \kappa_0 \frac{(C_k Q_k)^3 (1 - I_k)}{(\bar{t}_k^c)^2} \\ & \text{Subject to} \quad \sum_{k=1}^K I_k R_k \leq S, \quad I_k = \{0, 1\}, \forall k \in \mathcal{K}. \end{aligned}$$

Remark 6.2: The ILP problem (P2-2), despite of being exponentially complex in the worst case, admits on average complexity of $\mathcal{O}(L^2 \log L)$ thanks to the recently developed fast branch and bound method, e.g., Lenstra-Lenstra-Lovasz (LLL) algorithm [30], which can be effectively solved using off-the-shelf software packages, e.g., [31].

Although this proposed suboptimal cache placement is on average of lower complexity than the optimal cache placement obtained via solving (P2-1) ($\mathcal{O}(2^{|\mathcal{S}|})$) using exhaustive search, it assumes that each computation task offloaded to the edge server adopts the maximum computation frequency f_0^{max} , which leads to larger computation energy consumption at the edge server.

Moreover, this suboptimal solution does not apply to problem (P0'), where there are in general no close-form for α_l^{off} and α_l^{off} , for $s_l \in \mathcal{S}$.

VII. NUMERICAL RESULTS

In this section, we verify the effectiveness of our proposed deep learning based service cache placement algorithms for problem (P0) as well as the suboptimal cache placement designed for the special-case problem (P1). We consider a wireless setup where there are $K = 5$ locations deployed on a circle with radius $d_k = d = 0.03$ km centered on the BS, $\forall k \in \mathcal{K}$, and a service library with $L = 10$ types of services. A task request from location $k \in \mathcal{K}$ follows Zipf distribution given by [32]

$$P_{l,k} = \frac{1}{l_k^{\sigma_k}} \left(\sum_{s_l \in \mathcal{S}} \frac{1}{l_k^{\sigma_k}} \right)^{-1}, \quad (41)$$

where σ_k determines the skewness of the preference profile at location k , and $l_k = \pi_k(l)$ is the rank of service $s_l \in \mathcal{S}$ in terms of popularity at location k , represented by a permutation $\pi_k(\cdot)$ over $\{1, \dots, L\}$. The average channel gain A_0 is set as 128.1 dB at reference distance $d_0 = 1$ km with the pathloss exponent factor $\gamma = 2.6$. The Rayleigh fading is generated by *i.i.d.* complex Gaussian RVs with zero mean and unit variance. The task-input and task-output bit-lengths follow uniform distributions, denoted by $Q_l \sim \mathcal{U}[\frac{4}{15}, \frac{1}{3}]$ Mbits and $R_l \sim \mathcal{U}[0.7, 1]$ Mbits, $s_l \in \mathcal{S}$. Other parameters are set as follows unless otherwise specified: transmission BW $B_{\text{off}} = B_{\text{dl}} = 2$ MHz, noise spectrum density $N_0 = -169$ dBm/Hz, weighted factors for problem (P0) $\beta_0 = 0.5$, $\beta_k = 0.5/K$, the maximum edge server's computation frequency $f_0^{\text{max}} = 10$ GHz, transmission power $p_k^{\text{off}} = 0.25$ W, $p_l^{\text{dl}} = 1$ W, capacitance coefficient $\kappa = 10^{-27}$, and the number of CPU cycles required for computation service s_l $C_l = 1000$ cycles/bit, $\forall k \in \mathcal{K}, s_l \in \mathcal{S}$. Furthermore, the deadline for each task is set to be the same, e.g., $T_l = T = 0.8$ s, $\forall s_l \in \mathcal{S}$.

As benchmarks, we consider the optimal cache placement using exhaustive search as well as other benchmarks for all the problems as follows.

- **Greedy caching:** The main idea of the greedy cache placement scheme is to exploit to the maximum extent the caching capacity S . Specifically, we initially set all the tasks as $I_l = 0, \forall s_l \in \mathcal{S}$. Then, we solve (P0'-1) to obtain the weighted-sum expected energy consumption. Next, we set the cache placement of the \bar{l} th service with the largest energy consumption as $I_{\bar{l}} = 1$. Then we repeat the above procedure until constraint (3) is feasible. This heuristic algorithm is summarized in Algorithm 3.

- **Popular caching:** We cache the most popular services as per the preference profile for locations in \mathcal{K} . First, we calculate the probability of being request for each service $s_l \in \mathcal{S}$, i.e., $1 - \Pr(|\mathcal{K}_l| = 0)$ and order these probability in descending order. Then we cache in descending order the results of those services until the constraint (3) is violated.
- **No caching:** All task results are not cached, and each task on demand has to be offloaded to and executed at the edge server.
- **All caching:** This scheme assumes no constraint (3), so all task results are cached at the edge server. It serves as the performance upper-bounds for all other schemes.

Algorithm 3: Greedy Cache Placement Scheme

Initialize: $\mathbf{I}^{(0)} = [0, \dots, 0]^T$, $\mathcal{S}^{(0)} = \mathcal{S}$ and $n = 0$

1 **repeat**

2 Solve (P0'-1) to obtain service s_l 's expected energy consumption

$$E_l = \beta_0(\mathbb{E}[E_l^c] + E_l^{\text{dl}}) + \sum_{k=1}^K \beta_k \mathbb{E}[E_{k,l}^{\text{off}}], \forall s_l \in \mathcal{S}^{(n)};$$

3 Set $I_{\bar{l}}^{(n)} = 1$ for service $\bar{l} = \arg \max_{s_l \in \mathcal{S}^{(n)}} E_l$;

4 Update $\mathcal{S}^{(n+1)} = \mathcal{S}^{(n)} \setminus s_{\bar{l}}$;

5 Update $n = n + 1$.

6 **until** Constraint (3) is infeasible;

Output : $\mathbf{I}^{(n)}$

A. DL Based Offline Cache Placement for (P0)

For the DL based offline cache placement, we consider the offline learning problem (P1) using a fully connected DNN (c.f. Fig. 1) that consists of one input layer, three hidden layers, and one output layer, where the first, second and third hidden layers have 160, 120, and 80 hidden neurons, respectively. We implement the algorithm in Matlab R2020a 9.8 using Deep Learning Toolbox 14.0 and set the learning rate $\eta^{(t)} = 0.01$, mini-batch size for training $|\mathcal{D}^{(t)}| = 128$, $\forall t$, the memory size $|\mathcal{R}|$ as 1024, and the training interval $\tau = 10$. We use channel gains and task input/output bits distributed as above to simulate the input data coming of DNN. In addition to the benchmarks described above, we also evaluate the performance of the ‘‘DL-based caching with order-preserving quantization’’, in which the order-preserving quantization preserves the ordering of all the entries in a vector during quantization [22].

Fig. 3 and Fig. 4 illustrate the convergence performance of the deep learning based cache placement algorithms with different quantization methods using offline implementation. It is observed from Fig. 3 that both training loss of the DNN with different quantization methods decrease and become stable as time progresses, whose fluctuation is mainly owing to the random sampling of training data. It is worth noting that the algorithm with stochastic quantization method not only wins in training loss, but it is also more robust as the deviation is much smaller. Furthermore, we verify the effectiveness of the trained DNN, whose test loss is demonstrated in Fig. 4. It is seen that as time goes by, both test losses decline and the one with stochastic quantization method outperforms the other due to the random exploration of the service caching decisions space.

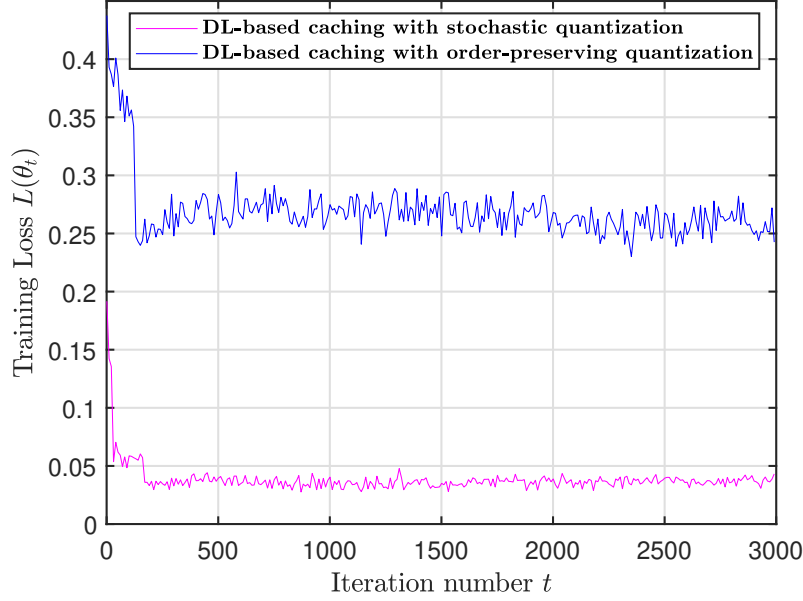


Fig. 3. The training loss versus the iteration number.

In Fig. 5, we plot the expected weighted-sum energy versus the caching capacity constraint for all caching schemes. It is seen that the expected weighted-sum energy of all schemes drops with the caching capacity. This is intuitively true, as larger caching capacity can accommodate more service results at the edge server. Thanks to the larger diversity brought by the proposed noise-aided stochastic quantization, the cache placement employing the stochastic quantization outperforms all the other benchmarks, approaching the “Optimal caching” when the caching capacity increases. In particular, when the caching capacity exceeds 8.5 Mbits, all schemes overlap

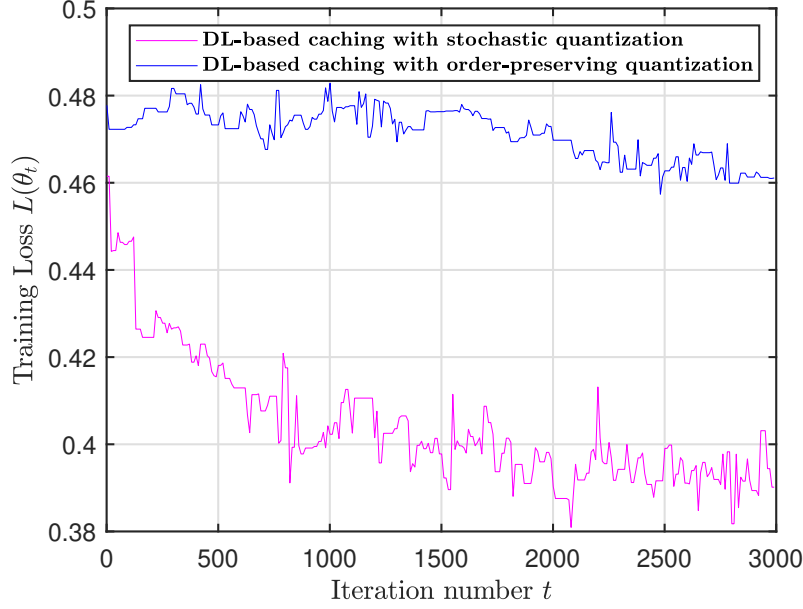


Fig. 4. The test loss versus the iteration number.

with the “All caching” scheme, since sufficiently large capacity always satisfy $\sum_{s_l \in S} R_l < S$, enabling the trivial case of $I_l^* = 1, \forall s_l \in S$. In addition, all the shown caching schemes significantly surpass the “No caching” one, which yields the expected weighted-sum energy as high as 0.3727 Joule.

The expected weighted-sum energy versus the computation deadline T for different cache placement schemes is shown in Fig. 6. The weighted-sum energy for all the schemes gradually goes down when the deadline is extended, since more tolerant deadline allows longer execution time for services, thus saving the computation energy E^c (c.f. (9)). In addition, the proposed offline caching with stochastic quantization performs the best among all the suboptimal schemes thanks to the random exploration of the caching capacity, while the one with order-preserving quantization is just slightly better than “Popular caching” and “Greedy caching” methods. Similar to Fig. 5, “No caching” yields the largest expected weighted-sum energy consumption among all the schemes, which is shown in the table in Fig. 6.

Fig. 7 shows the expected weighted-sum energy consumption for different number $|\mathcal{S}|$ of services with $K = 5$ locations. The expected weighted-sum energy consumed by all the schemes increases with the total number of services. The performance gap between the proposed offline caching with stochastic quantization and all the other suboptimal caching schemes enlarges

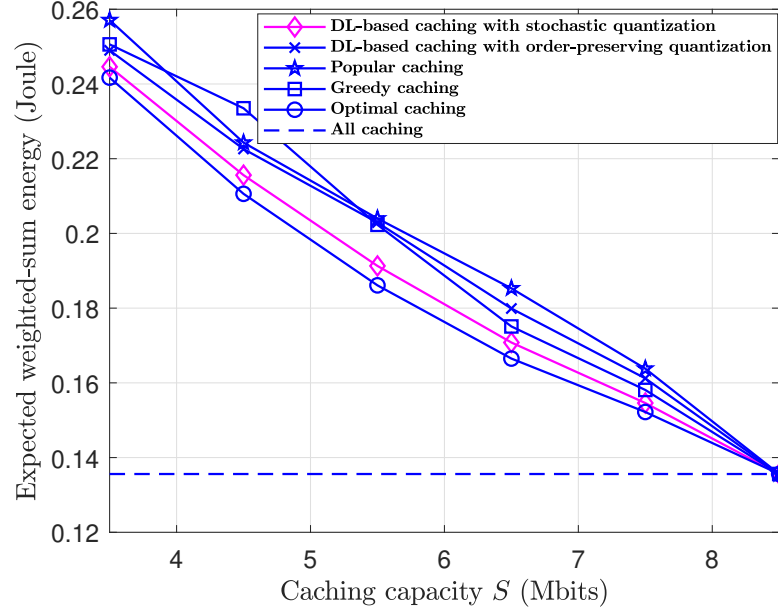


Fig. 5. The expected weighted-sum energy versus the caching capacity constraints.

Deadline T (s)	0.8	0.9	1.0	1.1	1.2	1.3	1.4	1.5
"No caching" energy (Joule)	0.3727	0.2981	0.2549	0.2276	0.2093	0.1963	0.1869	0.1798

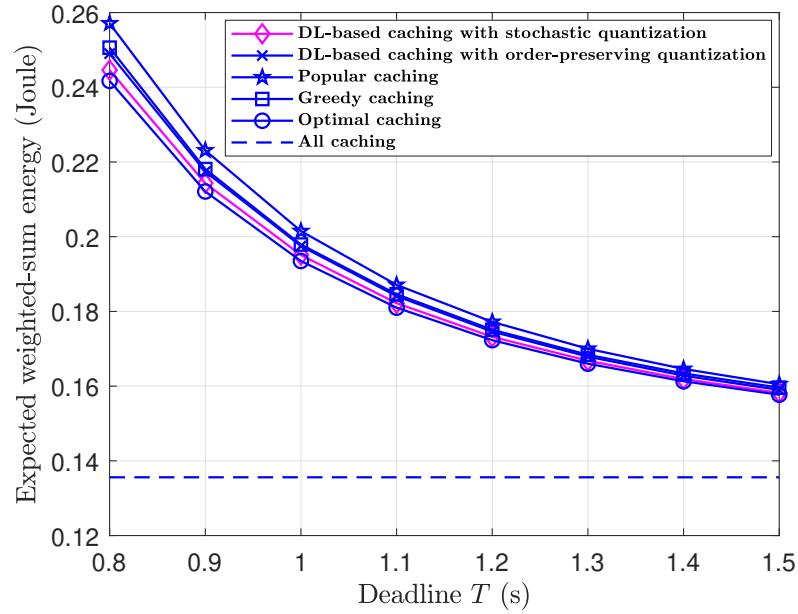


Fig. 6. The expected weighted-sum energy versus the deadline constraints with $S = 3.5$ Mbits.

with the number $|\mathcal{S}|$ of services. Specifically, the proposed caching schemes saves 6.12% of energy when there are $|\mathcal{S}| = 10$ services versus 1.82% when $|\mathcal{S}| = 6$, showing the promising performance of the proposed caching scheme for large $|\mathcal{S}|$. Furthermore, the proposed caching scheme is seen to approach the “Optimal caching” with little gap for all values of $|\mathcal{S}|$.

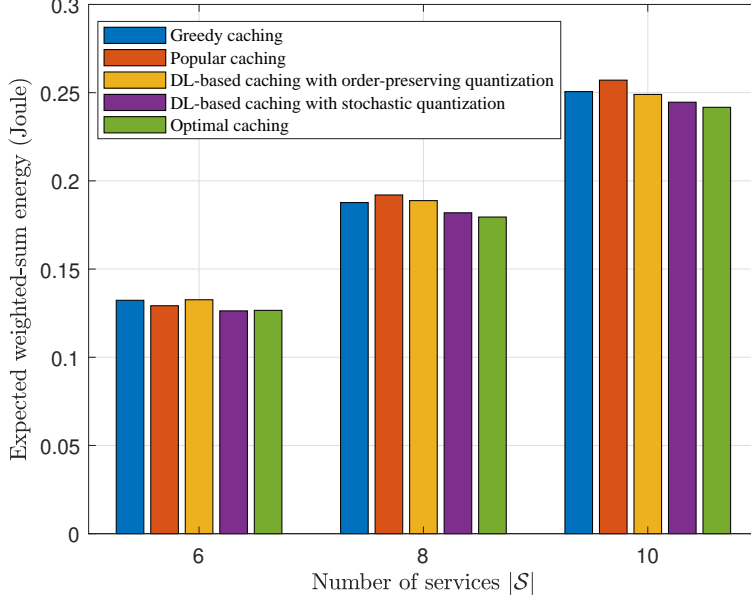


Fig. 7. The expected weighted-sum energy versus the total number of services with $S = 3.5$ Mbits.

B. ILP-based Suboptimal Cache Placement for (P2)

In this subsection, we evaluate the performance of the ILP-based caching scheme proposed in section IV as compared against “No caching”, “All caching” as well as “Optimal caching”. The parameters considered in this subsection is the same as those in Section VII-A.

Fig. 8 shows the expected weighted-sum energy versus the caching capacity constraint achieved by different caching schemes. As seen in the general case in Section VII-A, except for the “No caching”, the weighted-sum energy of all schemes declines with the caching capacity constraint, approaching the all caching scheme with $I_l^* = 1, \forall s_l \in \mathcal{S}$, when S is larger than around 8 Mbits. Additionally, “No caching” is outperformed by all the other caching based schemes as expected.

Next, we demonstrate the expected weighted-sum energy versus the deadline constraints T in Fig. 9. It shows that the ILP-based caching scheme achieves near-optimal performance especially when the deadline constraint T is sufficiently long. This is because longer deadline T allows

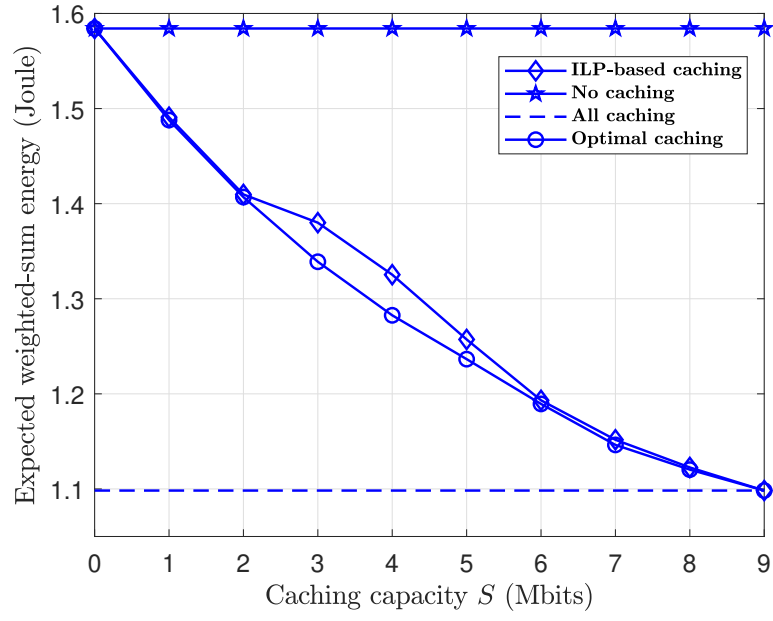


Fig. 8. The expected weighted-sum energy versus the caching capacity constraint.

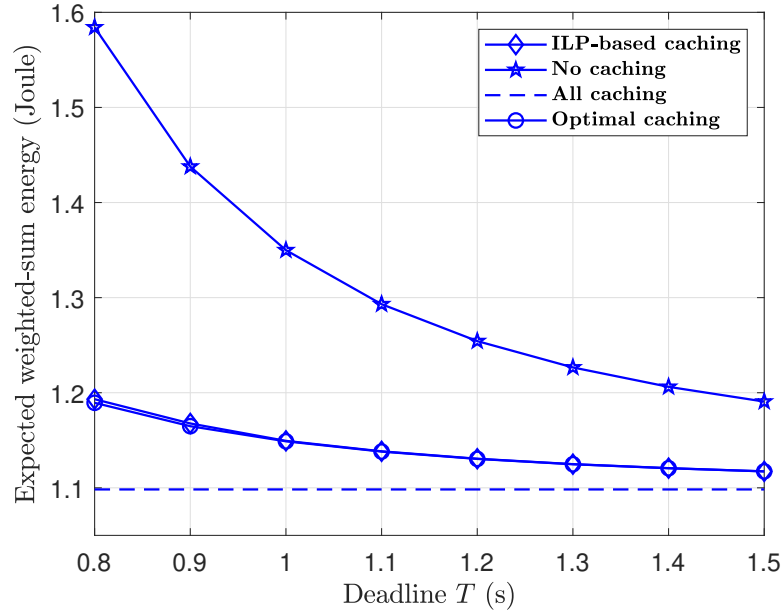


Fig. 9. The expected weighted-sum energy versus the deadline constraints with $S = 6$ Mbits.

less computation time, thus leading to lower energy consumption E^c . In addition, the expected weighted sum energy consumption of the “All caching” scheme remains nearly unchanged, since all services have already been cached at the edge server and therefore extending deadline T won’t help saving computation energy E^c as the other schemes in Fig. 9.

VIII. CONCLUSION

In this paper, we considered a multi-user service-caching enabled MEC system, which serves multiple representative locations with the users at each of them being of a typical preference profile over the given set of computation services. In a FDMA setup, we formulated a joint resource allocation and cache placement optimization problem to minimize the expected weighted-sum energy of the edge server and the users with respect to the location-dependent preference profiles, subjected to the computation, bandwidth and caching capacities as well as the service latency constraints. Under the assumption of known distributions of the channel gains and the task input/output bit-length, we proposed a DL-based service cache placement framework to tackle the mixed-integer challenges, where a DNN is trained offline and then used to predict caching decisions. To achieve better training performance, we also improved the exploration during training by employing a novel stochastic quantization based caching decision generation scheme. Finally, numerical results showed the striking performance achieved by service caching, in particular, the proposed DL-based service cache placement using stochastic quantization.

APPENDIX I

PROOF OF LEMMA OF 4.1

Given a set of (feasible) dual variables, we solve problem (27a)-(27c) for their corresponding variables using some of the Karush-Kuhn-Tucker (KKT) conditions [26] as follows.

$$\begin{aligned}
 & -2\beta_0\kappa_0(1 - \bar{I}_l)\frac{(C_l Q_l)^3}{(t_l^c)^3}(1 - \prod_{k=1}^K(1 - P_{l,k})) + \mu_l - \eta_l = 0, \forall s_l \in \mathcal{S}. \\
 & \begin{cases} \beta_0 p_l^{\text{dl}} P_{l,\pi(k)}^{\text{dl}} - \gamma_{l,k} \frac{R_l}{(t_{l,\pi(k)}^{\text{dl}})^2} = 0, & \forall s_l \in \mathcal{S}, k \in \mathcal{K} \setminus \{K\}, \\ \beta_0 p_l^{\text{dl}} P_{l,\pi(k)}^{\text{dl}} + \mu_l - \gamma_{l,k} \frac{R_l}{(t_{l,\pi(k)}^{\text{dl}})^2} = 0, & \forall s_l \in \mathcal{S}, k = K. \end{cases} \\
 & \begin{cases} \beta_k p_k^{\text{off}} P_{l,k}^{\text{off}} - \omega_{l,k} \frac{Q_l}{(t_{l,k}^{\text{off}})^2} = 0, & \forall s_l \in \mathcal{S}, k \in \mathcal{K} \setminus \{K\}, \\ \beta_k p_k^{\text{off}} P_{l,k}^{\text{off}} + \mu_l - \omega_{l,k} \frac{Q_l}{(t_{l,k}^{\text{off}})^2} = 0, & \forall s_l \in \mathcal{S}, k = K. \end{cases}
 \end{aligned}$$

After some manipulations, we obtain the optimal solution to (27a)-(27c). Similarly, (38a)-(38e) can also be obtained as above.

REFERENCES

- [1] J. Chen, H. Xing, X. Lin and S. Bi, "Joint cache placement and bandwidth allocation for FDMA-based mobile edge computing system," *IEEE ICC 2020*, Jun. 2020.
- [2] M. Chiang and T. Zhang, "Fog and IoT: An overview of research opportunities," *IEEE Internet Things J.*, vol. 3, no. 6, pp. 854-864, Dec. 2016.
- [3] L. Liu, S. Bi and R. Zhang, "Joint power control and fronthaul rate allocation for throughput maximization in OFDMA-based cloud radio access network," *IEEE Trans. Commun.*, vol. 63, no. 11, pp. 4097-4110, Nov. 2015.
- [4] Y. Mao, C. You, J. Zhang, K. Huang, and K. B. Letaief, "A survey on mobile edge computing: The communication perspective," *IEEE Commun. Surveys Tuts.*, vol. 19, no. 4, pp. 2322-2358, 4th Quart. 2017.
- [5] L. Pu, X. Chen, J. Xu and X. Fu, "D2D fogging: An energy-efficient and incentive-aware task offloading framework via network-assisted D2D collaboration," *IEEE J. Sel. Areas Commun.*, vol. 34, no. 12, pp. 3887-3901, Dec. 2016.
- [6] H. Xing, L. Liu, J. Xu and A. Nallanathan, "Joint task assignment and resource allocation for D2D-enabled mobile-edge computing," *IEEE Trans. Commun.*, vol. 67, no. 6, pp. 4193-4207, Jun. 2019.
- [7] S. Bi and Y.-J. Zhang, "Computation rate maximization for wireless powered mobile-edge computing with binary computation offloading," *IEEE Trans. Wireless Commun.*, vol. 17, no. 6, pp. 4177-4190, Jun. 2018.
- [8] F. Wang, J. Xu, X. Wang, and S. Cui, "Joint offloading and computing optimization in wireless powered mobile-edge computing system," *IEEE Trans. Wireless Commun.*, vol. 17, no. 3, pp. 1784-1797, Mar. 2018.
- [9] S. Sardellitti, G. Scutari, and S. Barbarossa, "Joint optimization of radio and computational resources for multicell mobile-edge computing," *IEEE Trans. Signal Inf. Process. Over Netw.*, vol. 1, no. 2, pp. 89-103, Jun. 2015.
- [10] F. Wang, H. Xing and J. Xu, "Real-Time resource allocation for wireless powered multiuser mobile edge computing with energy and task causality," *IEEE Trans. Commun.*, vol. 68, no. 11, pp. 7140-7155, Nov. 2020.
- [11] X. He, H. Xing, Y. Chen and A. Nallanathan, "Energy-efficient mobile-edge computation offloading for applications with shared data," in *Proc. IEEE Global Communications Conference (GLOBECOM)*, Abu Dhabi, UAE, Dec. 2018.
- [12] S. Bi, L. Huang and Y. J. Zhang, "Joint optimization of service caching placement and computation offloading in mobile edge computing system," *IEEE Trans. Wireless Commun.*, vol. 19, no. 7, pp. 4947-4963, Jul. 2020.
- [13] H. Xing, J. Cui, Y. Deng, and A. Nallanathan, "Energy efficient proactive caching for fog computing with correlated task arrivals," in *Proc. IEEE 20th Int. Workshop Signal Process. Adv. Wireless Commun.*, Cannes, France, July 2019.
- [14] Y. Cui, W. He, C. Ni, C. Guo and Z. Liu, "Energy-efficient resource allocation for cache-assisted mobile edge computing," in *Proc. IEEE Local Comput. Netw.*, Singapore, Oct. 2017, pp. 640-648.

- [15] Y. Sun, Z. Chen, M. Tao and H. Liu, "Bandwidth gain from mobile edge computing and caching in wireless multicast systems," *IEEE Trans. Wireless Commun.*, vol. 19, no. 6, pp. 3992-4007, Jun. 2020.
- [16] W. Wen, Y. Cui, T. Q. S. Quek, F-C Zheng and S. Jin, "Joint optimal software caching, computation offloading and communications resource allocation for mobile edge computing," *IEEE Trans. Veh. Technol.*, vol. 69, no. 7, pp. 7879-7894, Jul. 2020.
- [17] A. Ndikumana *et al.*, "Joint communication, computation, caching, and control in big data multi-access edge computing," *IEEE Trans. Mobile Comput.*, vol. 19, no. 6, pp. 1359-1374, Jun. 2020.
- [18] S. Zhang and J. Liu, "Optimal probabilistic caching in heterogeneous IoT networks," *IEEE Internet Things J.*, vol. 7, no. 4, pp. 3404-3414, Apr. 2020.
- [19] M. Tao, E. Chen, and H. Zhou, "Content-Centric Sparse Multicast Beamforming for Cache-enabled Cloud RAN," *IEEE Trans. Wireless Commun.*, vol. 15, no. 9, pp. 6118-6131, 2016.
- [20] Y. Sun, Y. Cui, and H. Liu, "Joint pushing and caching for bandwidth utilization maximization in wireless networks," *IEEE Trans. Commun.*, vol. 67, no. 1, pp. 391-404, Jan. 2019.
- [21] S. Mller, O. Atan, M. van der Schaar and A. Klein, "Context-aware proactive content caching with service differentiation in wireless networks," *IEEE Trans. Wireless Commun.*, vol. 16, no. 2, pp. 1024-1036, Feb. 2017.
- [22] L. Huang, S. Bi, and Y. J. Zhang, "Deep reinforcement learning for online computation offloading in wireless powered mobile-edge computing networks," *IEEE Trans. Mobile Comput.*, vol. 19, no. 11, Nov. 2020.
- [23] K. Guo, M. Sheng, T. Q. S. Quek and Z. Qiu, "Task offloading and scheduling in fog RAN: A parallel communication and computation perspective," *IEEE Wireless Commun. Letters*, vol. 9, no. 2, pp. 215-218, Feb. 2020.
- [24] G. Lee, W. Saad and M. Bennis, "An online optimization framework for distributed fog network formation with minimal latency," *IEEE Trans. Wireless Commun.*, vol. 18, no. 4, pp. 2244-2258, Apr. 2019.
- [25] U. Cho, T. Kim, Y. Yoon, J. Lee et al., "A 1.2-V 1.5-Gb/s 72-Mb DDR3 SRAM " *IEEE Journal of Solid-State Circuits*, vol. 38, no. 11, pp. 1943-1951, Nov. 2003.
- [26] S. Boyd and L. Vandenberghe, "Convex Optimization." Cambridge, U.K.: Cambridge Univ. Press, 2004.
- [27] S. Boyd, "Lecture Notes for EE364b: Convex Optimization II." [online]. Available: <https://stanford.edu/class/ee364b/lectures.html>
- [28] M. Grant and S. Boyd. (2014). *CVX: MATLAB Software for Disciplined Convex Programming. Version 2.1*. [online]. Available: <http://cvxr.com/cvx>
- [29] R. Corless, G. Gonnet, D. Hare, D. Jeffrey, and D. Knuth, "On the Lambert W function," *Adv. Comput. Math.*, vol. 5, no. 1, pp. 329-359, Dec. 1996.
- [30] M. Jünger, *et al.*, Eds., "50 Years of interger programming 1958-2008: From the early years to the state-of-the-art." New York, NY, USA: Springer, 2010.
- [31] Gurobi Optimization [online]. Available: <http://www.gurobi.com/>
- [32] S. Tamoor-ul-Hassan, M. Bennis, P. H. J. Nardelli and M. Latva-aho, "Caching in wireless small cell networks: A storage-bandwidth tradeoff," *IEEE Commun. Lett.*, vol. 20, no. 6, pp. 1175-1178, Mar. 2016.